# SYNTHESIS AND CHARACTERIZATION OF SEMICONDUCTORS VIA TWO ROUTES: COORDINATION FRAMEWORKS AND METAL ORGANIC FRAMEWORKS

by

GREGORY DYE

THOMAS P. VAID, COMMITTEE CHAIR
SHANLIN PAN
GREGORY J. SZULCZEWSKI
DAVID E. NIKLES
TIM MEWES

A THESIS

Submitted in partial fulfillment of the requirements
for the degree of Master of Science
in the Department of Chemistry
in the Graduate School of
The University of Alabama

TUSCALOOSA, ALABAMA

2012

# ABSTRACT

The extension of the Creutz-Taube ion into an extended framework composed of mixed-valence ruthenium metal centers bridged by pyrazine organic spacers is described starting from pyrazine containing ruthenium precursors. The synthesis of a novel ruthenium(III) complex, $[RuCl_2(pyz)_4][BF_4]$ (where pyz = pyrazine), is described. The reaction of ruthenium precursors at high temperatures in a sealed reactor vessel yields a semiconducting, crystalline material, believed to be either a one- or two-dimensional network of ruthenium metal centers bridged by pyrazine, and is currently being studied under synchrotron x-ray diffraction experiments in order to determine the structure. The synthesis of cobalt precursors for an analogous experiment to form cobalt-based frameworks is reported. The synthesis of a novel anthracene-based protected tetrathiol is described, and reactions metal salts in various solvents to form extended frameworks has been attempted. Progress on the synthesis of alkyl-protected benzene selenols is reported, and initial reactions with lead salts are described.

# DEDICATION

This thesis is due to the encouragement and advice of a great many people. I would like to thank my fiance, Leslie Gentry, for all of her help and support, and my many friends who sought to guide and support me throughout my journey. The two people who deserve the most gratitude, who got me where I am today, and who I will always owe more than I can ever repay are my parents. This thesis is dedicated to them, since without them, I would not be who I am today.

(Y) and ZAX.

LIST OF ABBREVIATIONS AND SYMBOLS

| | | | |
|---|---|---|---|
| CF | coordination framework | MOF | metal organic framework |
| HOMO | highest occupied molecular orbital | LUMO | lowest unoccupied molecular orbital |
| $G_x$ | free energy plot of state x | $E_{op}$ or $\lambda$ | reorganization parameter |
| $H_{ab}$ | electronic coupling element | SOMO | singly occupied molecular orbital |
| pyz | pyrazine | UV-Vis | ultraviolet-visible |
| NIR | near-infrared | $E_g$ | band gap energy |
| DMSO | dimethylsulfoxide | hν | irradiation |
| equiv | equivalents | pyr | pyridine |
| NMR | nuclear magnetic resonance | G | conductance |
| I | current | V(V) | voltage |
| Vol($cm^3$) | volume | A | area |
| L | length of sample | σ | conductivity |
| triflate | trifluoromethanesulfonate | $Et_2O$ | diethyl ether |
| MeCN | acetonitrile | p-TsOH | p-toluenesulfonic acid |
| DMF | dimethylformamide | DMI | 1,3-dimethyl-2-imidazolidinone |
| TEA | triethylamine | TMEDA | tetra(methyl)ethylene diamine |
| bim | benzimidazolate | EI | electron ionization |
| MS | mass spectrometry | APCI | atmospheric pressure chemical ionization |

ACKNOWLEDGMENTS

I would like to thank Dr. Thomas P. Vaid for his support and guidance. He has allowed me to grow as a synthetic chemist in his group, and my knowledge base has expanded significantly under his mentorship.

I would also like to thank Dr. Gregory Szulczewski, Dr. Shanlin Pan, Dr. David Nikles, and Dr. Tim Mewes for serving on my committee and answering all of my questions. They have all excelled as committee members and have been instrumental in my learning experience. Dr. Gregory Szulczewski also deserves thanks for serving as my literature seminar advisor, and helping me learn more than I ever thought I would about field effect transistors.

There are many staff who I could not have succeeded without. I would like to thank Dr. Ken Belmore for all of his help. He is not only an excellent NMR spectroscopist, but is amazingly supportive of the graduate students and genuinely cares about everyone. Janice Voss, Evelyn Jackson, Carolyn Walker, and Reda Arnold are not only happy, supportive, helpful, and amazing, but always made my day better, and tried as hard as they could to get me whatever I needed. No one could ask for better office staff, and they go above and beyond what is expected of them just because they enjoy what they do. Rick Smith also deserves credit, for without his assistance, I would be in debt up to my eyeballs due to the glassware that he somehow manages to fix, even when it looks hopeless. I would like to thank Dr. Qiaoli Liang for mass spectrometry analysis of samples. I would also like to thank Dr. Peter Stephens for his analysis of synchrotron x-ray diffraction data.

The graduate students who have supported me are without compare, and I only hope I can be as helpful to them as they are to me. I cannot thank everyone, or it would double the size of this thesis, but special thanks need to go to a few. My fiancé, Leslie Gentry, will always have a special spot in my heart, and I love her more than can be expressed . Jane Moore and I have lived too many of the same experiences in life, and we understand each other too well. Caleb Hill and Edward Ellingsworth will always be amazing men, who deserve way more credit than they get for being good and true friends. Amanda Glover and Joe Meany have gone through so much with me, and we have shared such good times, that I cannot even describe the bond that we have. I would also like to thank Jonathan Williamson for his help and friendship. It isn't often that someone gets to say that they enjoyed their life as fully as I have, but with the research, the friends, and the family that I have, it's hard not to be incredibly happy.

CONTENTS

LIST OF TABLES

LIST OF FIGURES

LIST OF SCHEMES

LIST OF CHARTS

LIST OF EQUATIONS

# CHAPTER 1

# COORDINATION FRAMEWORKS

## Introduction

The search for novel semiconductors is an important area of research, in that semiconductors are a necessary material for many of the technologies which underlie our society. Semiconductors have applications in computer circuits where it is beneficial to have ease of production. Semiconductors are also playing an increasing role in our society as novel sensor materials are required to detect analytes such as environmental contaminants, explosive vapors, and chemical toxins. These sensor materials benefit from ease of processability, and also benefit from a porous surface, and a change in electronic or optical properties during exposure to a given analyte. Many chemical modifications have been applied to organic sensor materials in order to make them more specific or sensitive to a certain analyte. Sensor materials, due to their exposure to atmospheric conditions, also require that they be stable under these conditions, which has imposed limits on many materials in the past.[1]

Another application of semiconductors, and one that has seen a large growth in recent years, is battery technology. This technology benefits by creating a material which is porous, conducting, and is stable during electrochemical processes.

With this is mind, there are two main classes of semiconductors, organic and inorganic. Some examples of organic semiconductors are rubrene, pentacene, polyacetylene, polythiophene, and polypyrrole, along with their functionalized derivatives. Organic semiconductors have the benefit of being soluble in many common organic solvents, which allows for simpler

processability in order to fabricate devices. Organic semiconductors also allow for customization of properties through functionalization of the organic backbone. This allows for the use of the wide range of chemical reactions to modify the semiconductors towards the application desired. One disadvantage of organic semiconductors is that they typically have lower electron and hole mobilities than their inorganic counterparts, which results in lower conductivities of the materials, and leads to these materials being less useful than they otherwise would be.

Inorganic semiconductors, such as silicon, titanium dioxide, and cadmium sulfide, typically have very high electron and hole mobilities in comparison to organic semiconductors due to the fact that they are usually an extended structure covalently bonded together. They also tend to have higher relative thermal and chemical stability. They are generally only modifiable through doping, which does not modify the selectivity of these materials. As such, the use of organic semiconductors in sensors has shown one way in which inorganic semiconductors need to be improved.

This research will focus on the synthesis of a new class of materials, hybrid inorganic-organic semiconductors. These materials combine the benefits of both classes, and will hopefully show a reduction in the disadvantages. Hybrid inorganic-organic materials can be subdivided into two fields, coordination frameworks (CFs), which will be the focus of this chapter, and metal organic frameworks (MOFs), which will be discussed in chapter 2. A coordination framework is defined as an extended array of metal centers bound to organic spacers by dative bonds.[2] This is differentiated from a metal organic framework, which is an extended solid, often in three dimensions, bound covalently to organic spacers.[2] The organic spacers used to form both of the frameworks are generally multidentate ligands.

Coordination frameworks, with the dative bonds between metal centers and organic units, should form more crystalline products due to the reversible nature of the dative bond formation. These dative bonds, however, may lead to more environmental susceptibility, for the same reason. In discussing CFs, my research will focus on mixed valence metal centers. Mixed valence materials have been present in the literature for many years, and a classification system for them is in place. This classification system was proposed by Melvin Robin and Peter Day in 1967.[3] They proposed to classify mixed valence compounds into three different classes, based on their electrical, magnetic, and spectroscopic properties. Class I represents compounds which exhibit no electron delocalization across mixed valence metal centers, due to significantly different ligand field strengths or coordination environments. Such compounds have individual metal centers where oxidation states are fixed and localized. One examples of this is silver oxide, which can more formally be referred to as $Ag(I)Ag(III)O_2$. The coordination geometry of the silver atoms localizes the oxidation states due to the fact that the silver(I) atoms are bound linearly to oxygen, while the silver(III) atoms are bound in a square planar coordination geometry, as shown in the paper by Yvon, et al.[4]

Class II compounds exhibit electron transfer between metal centers, but the oxidation states remain localized and distinguishable based on spectroscopic study of the ligands bound to and the solvent molecules surrounding the metal centers. Such compounds have distinguishable oxidation states for separate metal centers, but the properties of the compounds include a transition between the centers, referred to as an intervalence charge transfer. A representative example of a class II compound is the oxo-bridged manganese complex, $[(bipy)_2MnO_2Mn(bipy)_2]^{3+}$ studied by Cooper and Calvin.[5] The oxidation state is localized on the timescale of x-ray crystallography studies, such that the bond lengths are inequivalent in the

crystal structure. Electron transfer does occur, however, which is seen as a broad band in the infrared attributable to the intervalence charge transfer.

Class III compounds are compounds which exhibit electron delocalization across the metal centers and any intervening ligands where the oxidation states are no longer distinguishable as being on one metal center or the other. This is due to a ligand with excellent electronic communication bridging the metal centers, or metal centers in such close proximity that electrons can transverse between the two easily. These compounds are characterized predominantly by having no energy barrier to electron transfer, which is an important parameter in discussing the borderline cases between class II and class III, such as the Creutz-Taube ion which will be discussed in detail later. An example of a class III compound is the transition-metal chalcogenide studied by Brown, et al.[6] In $KCu_4S_3$, the copper atoms are all in equivalent positions in the crystal structure. The compound exhibits metallic reflectivity and conductivity. The magnetic susceptibility agrees with the susceptibility based on the expected hole concentration per molar volume for a free electron metal. These traits all point towards the compound displaying metallic properties, which is characteristic of a class III Robin-Day compound.

In discussing electron transfer, there have been many contributions made to the field including those made by Marcus,[7,8] Hush,[9,10] and others.[11] The theory of electron transfer first requires classification of the transfer as either an inner sphere or outer sphere process. An outer

$$Fe(CN)_6^{4-} + Fe(CN)_6^{3-} \rightarrow Fe(CN)_6^{3-} + Fe(CN)_6^{4-} \qquad \text{Eqn. 1.1}$$

sphere process, as shown in Equation 1.1, is one in which the electron transfer is not mediated by a bridging ligand, but in which the two reactants are left with their same coordination sphere

after the electron transfer is complete. An inner sphere reaction, as shown in Equation 1.2, is one in which the two reactant molecules form an activated complex which contains a ligand bridging

$$[Co(NH_3)_5Cl]^{2+} + [Cr(H_2O)_6]^{2+} + 6\ H_2O \rightarrow \qquad \text{Eqn. 1.2}$$

$$[Co(H_2O)_6]^{2+} + [CrCl(H_2O)_5]^{2+} + 5\ NH_3$$

the two metal centers.[11] The example shown in Equation 1.2 forms the activated complex $[(NH_3)_5CoClCr(H_2O)_5]^{4+}$. The outer sphere reactions, due to symmetry and solvent effects, are much simpler to describe, whereas the inner sphere reactions require more in depth discussion of solvent and ligand effects which can differ from reaction to reaction. In the discussion of mixed-valence extended solids, it is suitable to merely use the outer sphere reaction parameters to describe the mixed valence systems.

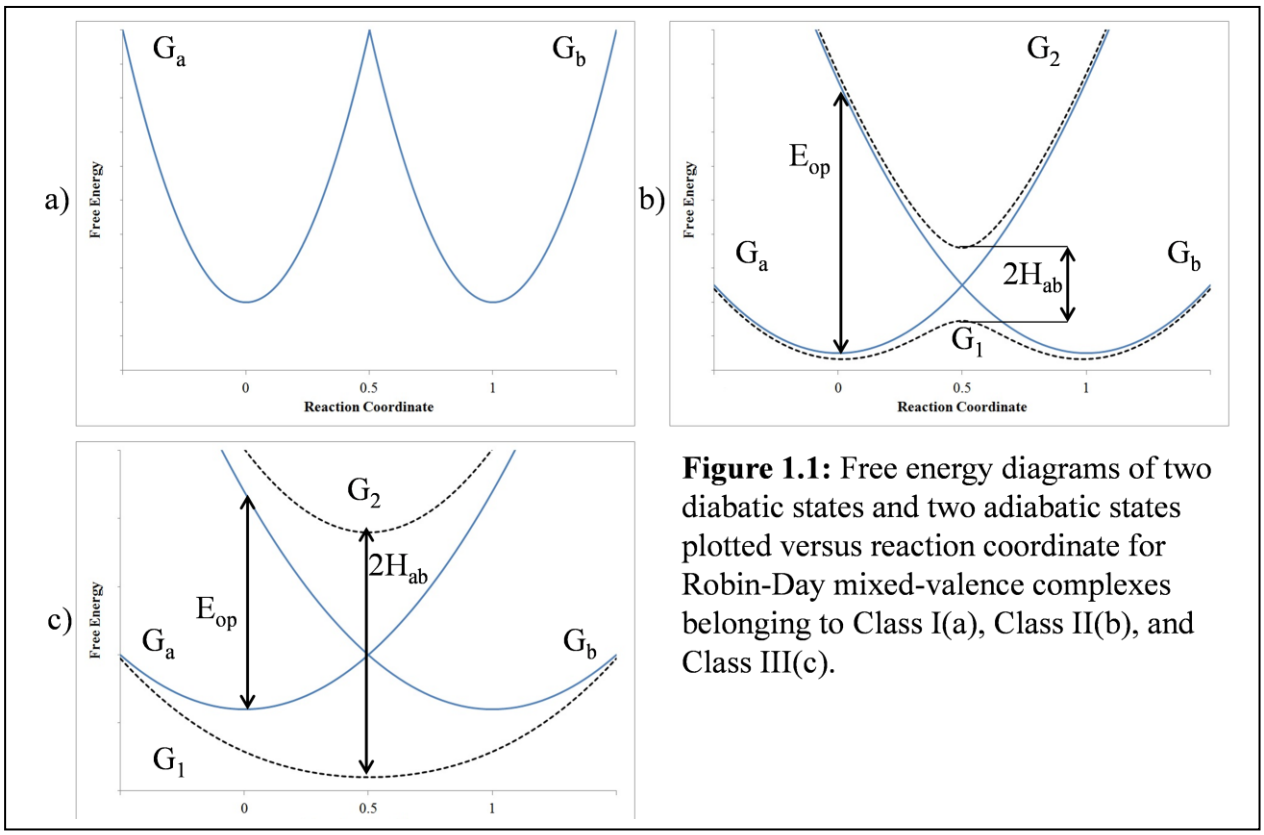


**Figure 1.1:** Free energy diagrams of two diabatic states and two adiabatic states plotted versus reaction coordinate for Robin-Day mixed-valence complexes belonging to Class I(a), Class II(b), and Class III(c).

There are a few terms that describe the electron transfer process and its likelihood to occur. These parameters are shown in Figure 1.1b, which shows a generic description of a class

II compound. The three different classes are shown in Figure 1.1. $G_a$ and $G_b$ are the diabatic states describing the free energy of the reactants and products separately. $G_1$ and $G_2$ are the adiabatic states formed from solving the two-state secular determinant for the reaction. $E_{op}$, or $\lambda$, is the reorganizational parameter which describes the difference between the free energies of the reactants and products at the equilibrium configuration of one or the other. $H_{ab}$ is the electronic coupling element, which describes the extent to which the electron delocalizes during the reaction. Class I compounds have no electron transfer under experimental conditions, which translates to the coupling element being very weak, essentially zero. As the coupling between the states increases, or $0<H_{ab}<\lambda/2$, the compound becomes a class II compound. When the electronic coupling becomes so great that $H_{ab}\geq\lambda/2$, the compound is classified as a class III compound. There is debate in recent literature deciding between whether compounds should fall into class II or class III when they are very close to the border.[12,13] In class II compounds, the solvent effects are localized due to the fact that the electron is localized on all timescales of solvent reorientations. In class III compounds, the solvent effects are averaged due to the fact that the electron is delocalized on all timescales of solvent reorientations. In the border line cases, which have recently become known as class II-III, the electron is delocalized on the timescale of frictional or diffusive solvent reorientations, such as a solvent molecule rotating to reverse its dipole towards the metal center. The electron is localized on the timescale of inertial solvent reorientations, such as bond lengthening and shortening. This leads to cases in which molecules have properties of both class II and class III compounds, such as the Creutz-Taube ion.

For complexes with a bridging ligand, it has been shown that including the free energy surface of the electron transfer to the bridging ligand in the reaction scheme also increases the

efficacy of describing the compound as either class II, "early" or "late" class II-III, or class III.[12] When using this three state model, there is an added transition, not only from metal to metal, but also from metal to bridging ligand. This helps to describe solvent and temperature effects that were previously not understood.

In discussing the states of the metal centers and bridging ligands, it is important to consider how this will affect the band structure of extended solids that are analogs of mixed-valence compounds. A class I material would be expected to be an insulator, since the large energy barrier for electron transfer between metal centers would translate into an insulator.

A class II material, having a lower energy barrier to electron transfer is expected to be a semiconductor. This energy requirement is mainly to change the local coordination environment around metal centers, such as shortening or lengthening of bonds between ligands and the metal. This small barrier translates to a small band gap in the semiconductor.

A class III material is expected to result in a metal, with a partially filled band in the band structure, shown generically in Figure 1.2. In terms of electron transfer, this is because the electron delocalization across metal centers should result in complete delocalization across the solid. There are splitting effects which could occur in an extended solid, from very simple to somewhat complex. One simple effect could be that a Peierl's distortion could take place, which would create a small band gap. More complicated effects could include strain, spin-splitting due to crystal deformities, and splitting of bands in crystals under applied or internal magnetic fields, which could cause the partially filled bands to split into a filled and an unfilled band, causing some

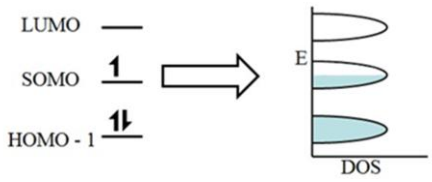


**Figure 1.2:** Expected transition from extension of molecular to extended solid for Robin-Day class III compounds.

extensions of class III molecules into extended solid analogs to form very small band gap semiconductors. These effects would be very interesting to study, but also could be used to develop further suitable materials for semiconductor applications.

The coordination frameworks designed will be extended analogs of the Creutz-Taube ion. The Creutz-Taube ion is an interesting mixed-valence species and provides an extremely good example of the debate over Robin-Day classification. The Creutz-Taube ion is a excellent representation of a symmetric mixed valence species where the bridging ligand provides excellent electronic communication between metal centers and the coordination environment doesn't change significantly between a Ru(II) and Ru(III) oxidation state. In 1969, Carol Creutz and Henry Taube published a study of $[(H_3N)_5Ru(pyz)Ru(NH_3)_5]^{n+}$ (where pyz = pyrazine and n = 4, 5, and 6).[14] The original study determined that the 5+ cation was a Ru(II)-Ru(III) complex, although future work pointed towards the fact that it should be instead classified as a $Ru^{2.5+}$-$Ru^{2.5+}$ complex. The investigation of the 4+ cation yields the expected Ru(II) absorption peaks in the ultraviolet-visible absorption spectrum, while the 6+ cation had the expected low intensity Ru(III) absorption spectrum. The UV-Vis absorption spectra are shown for all three complexes in Figure 1.3. Investigation of the 5+ cation, referred to as the Creutz-Taube ion

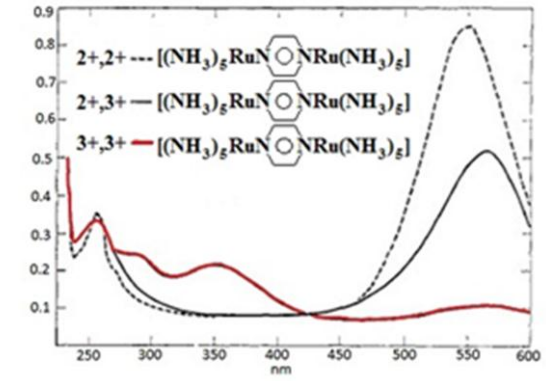


**Figure 1.3:** UV-Visible absorption spectra of $[(H_3N)_5Ru(pyz)Ru(NH_3)_5]^{n+}$.[14]

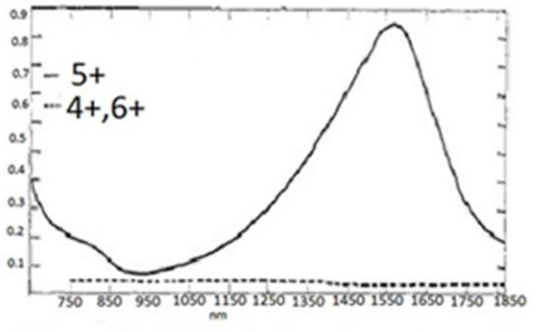


**Figure 1.4:** Near-infrared absorption spectra of $[(H_3N)_5Ru(pyz)Ru(NH_3)_5]^{n+}$. The dotted line is the blank, but is claimed to accurately represent the spectra of the 4+ and 6+ cations above 750 nm accurately.[14]

in future literature, yielded a slight shift in the maximum absorption from the 4+ cation but no new peaks appeared for the charge transfer transition. Creutz and Taube then investigated the near-infrared region and found a peak which could be attributed to the inter-valence charge transfer transition. The NIR spectra of the three complexes are shown in Figure 1.4. Future work on the peak shape and intensity found that the peak can be attributed to either a delocalized model, or a localized one, with some unique features.[13] This case actually falls very close to the borderline between class II-III and class III, in that there has been evidence of pressure dependence and presence of symmetrical ν(pyz) vibrations modes in the IR. The conclusions that can be drawn about the Creutz-Taube ion are that it is very close to delocalized in the ground state, and that spectroscopic data shows that it has a very likely potential for delocalization. It is this potential which has been studied when polynuclear ruthenium analogs have been studied,[15] and to which the coordination

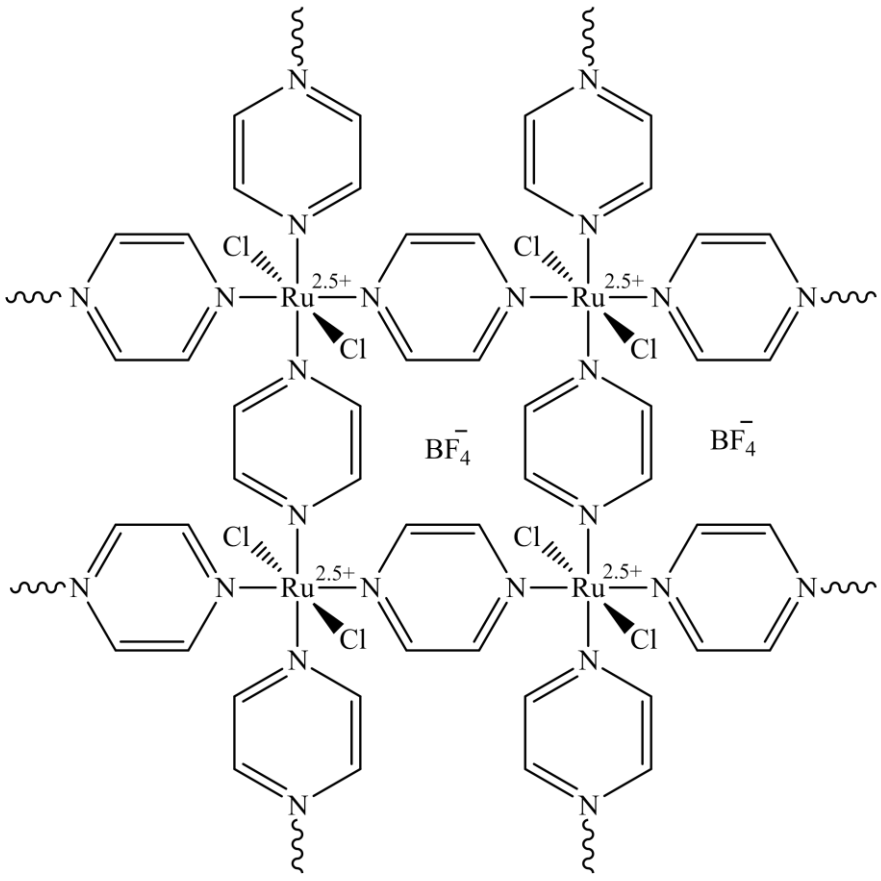


**Figure 1.5:** Expected geometry for ruthenium mixed-valence coordination framework.

framework project that I have studied will endeavor to recreate.

**Proposed Frameworks**

The extended analog of the Creutz-Taube ion which was intended is shown in Figure 1.5.

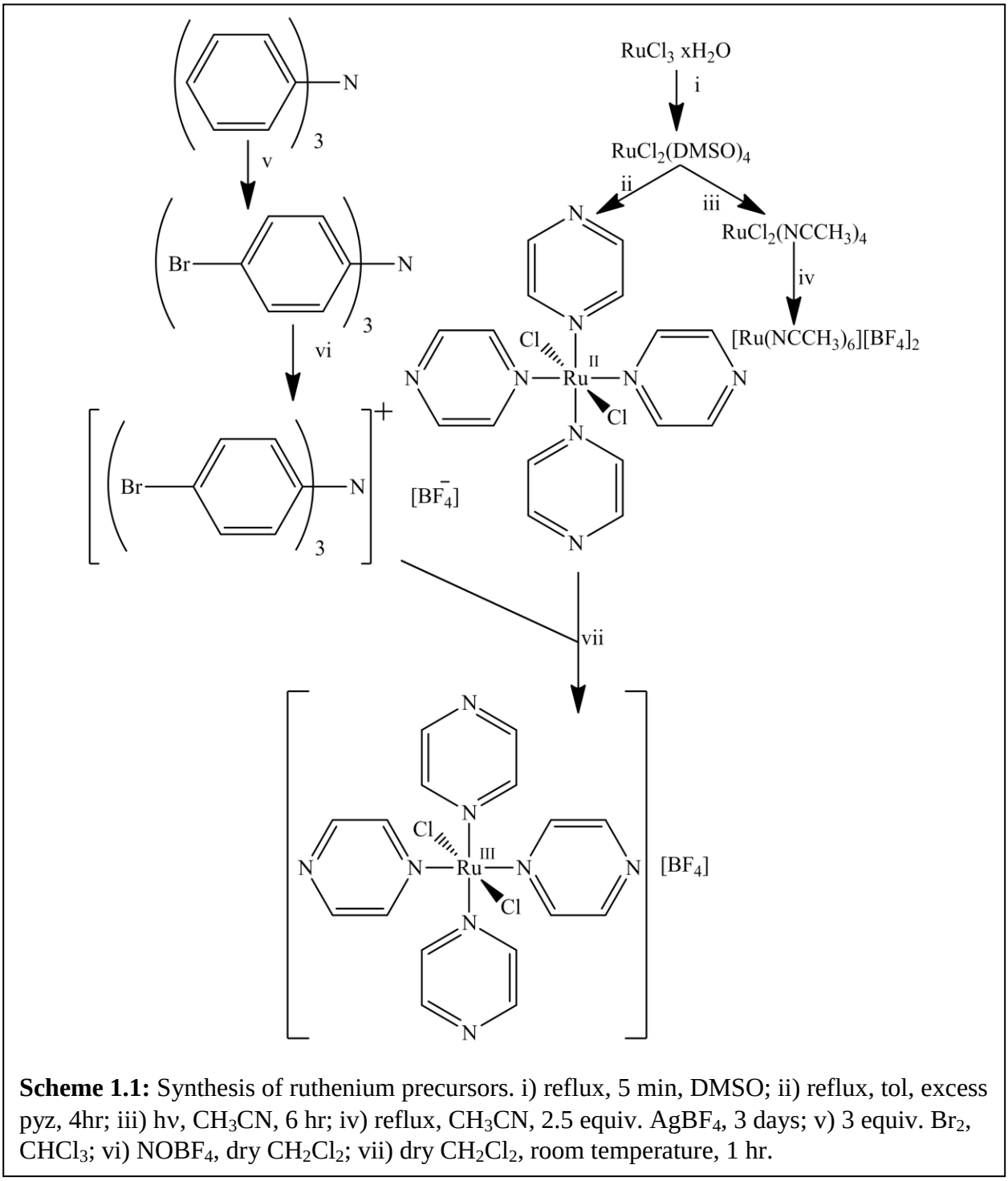


**Scheme 1.1:** Synthesis of ruthenium precursors. i) reflux, 5 min, DMSO; ii) reflux, tol, excess pyz, 4hr; iii) hν, $CH_3CN$, 6 hr; iv) reflux, $CH_3CN$, 2.5 equiv. $AgBF_4$, 3 days; v) 3 equiv. $Br_2$, $CHCl_3$; vi) $NOBF_4$, dry $CH_2Cl_2$; vii) dry $CH_2Cl_2$, room temperature, 1 hr.

The crystallinity of the desired product is important in order to allow for structural characterization in a straightforward manner.

In order to synthesize the desired product, mixed-valence precursors were required. The complete synthesis of ruthenium(II) and ruthenium(III) precursors has not been published, so an attempt was made to start from inexpensive starting materials and synthesize air-stable ruthenium precursors, which could then be combined to synthesize extended solids. Scheme 1.1 shows the route which was used to synthesize ruthenium(II) and ruthenium(III) precursors.

After the synthesis of the precursors, reactions were performed in order to identify which combination of starting materials and under which experimental conditions would yield a crystalline and semiconducting product that could be studied further.

The analogous project was intended to synthesize cobalt precursors which could then be used to form extended solids with cobalt instead of ruthenium in order to study the effect of substitution of a different metal center with the same bridging ligand. The synthesis of $[CoCl_2(pyr)_4][Cl]$ (where pyr = pyridine) was already present in the literature,[16] so the first path which seemed logical was to synthesize the cobalt(III) tetrapyridine complex with a non-coordinating anion and then proceed to substitute the pyridines with pyrazine. After that proved ineffective, synthesis of the cobalt(III) tetrapyrazine precursor directly was attempted.

**Results and Discussion**

*Ruthenium pyrazine networks*

The synthesis of some of the ruthenium(II) precursors for extended analogs of the Creutz-Taube ion were present in the literature. As shown in Scheme 1.1, steps i,[17] ii,[18] iii,[19] and v[20] were reported procedures, and step vi was an adaptation from existing literature.[21,22] Step vii was originally tried with $[SbCl_6]^-$ as the anion for the reaction, but it did not yield a pure product.

The final synthesis for $[RuCl_2(pyz)_4][BF_4]$ was found that yields a crystalline precipitate falling out of solution, which made isolation extremely simple. $^1$H-NMR of $[RuCl_2(pyz)_4][BF_4]$ showed no peaks, as would be expected due to peak broadening from the paramagnetic ruthenium metal center. UV-Vis spectroscopy showed a very weak absorption for $[RuCl_2(pyz)_4][BF_4]$, which was to be expected from the descriptions in the literature of other ruthenium(III) compounds. Single crystal diffraction is underway in order to fully characterize the structure.

$[RuCl_2(pyz)_4][BF_4]$ was then combined at various temperatures and in various solvents with multiple other ruthenium(II) compounds. $[RuCl_2(pyz)_4][BF_4]$ showed to be stable in solution, with $^1$H-NMR taken in deuterated solvent both in dark and in the light over multiple weeks showing no pyrazine disassociating from the compound. $RuCl_2(pyz)_4$, in comparison, showed a slow precipitation of a dark brown solid and a growth of a peak for unbound pyrazine occurring over the course of a few days to a week under the same conditions. For this reason, it was thought that a ruthenium(II) precursor in which the ligands cause the lower oxidation state to reside on that metal center would be advantageous for the formation of an extended solid. Lever's electrochemical series[23] was used as a comparison of ligand field effects in order to predict which ligands would be most advantageous. The compound $RuCl_2(DMSO)_4$, which was a precursor for the ruthenium(III) complex, was thought to be the best for this effect, in that the DMSO ligands on the ruthenium(II) metal center should disassociate and leave a coordination site for the pyrazine from $[RuCl_2(pyz)_4][BF_4]$. The reactions, shown in Equation 1.3, between $RuCl_2(DMSO)_4$ and $[RuCl_2(pyz)_4][BF_4]$, however, showed no crystallinity.

$$RuCl_2(DMSO)_4 + [RuCl_2(pyz)_4][BF_4] \rightarrow \qquad \text{Eqn. 1.3}$$

The reaction of $RuCl_2(NCCH_3)_4$ and $[RuCl_2(pyz)_4][BF_4]$ was then tried in hopes that the

$$RuCl_2(NCCH_3)_4 + [RuCl_2(pyz)_4][BF_4] \rightarrow \qquad \text{Eqn. 1.4}$$

acetonitrile ligand would be a weaker binding ligand than DMSO, and would thereby form a more crystalline framework. The reaction was refluxed for 24 hours and no precipitate formed.

This led to trials of $RuCl_2(pyz)_4$ and $[RuCl_2(pyz)_4][BF_4]$. Initially, $RuCl_2(pyz)_4$ was avoided as a ruthenium(II) precursor due to low solubility and apparent instability in solution, especially under light. Initially, the two ruthenium tetra(pyrazine) compounds were dissolved in

$$RuCl_2(pyz)_4 + [RuCl_2(pyz)_4][BF_4] \rightarrow \qquad \text{Eqn. 1.5}$$

acetonitrile and left at room temperature. No reaction was seen. At elevated temperatures in acetonitrile, the product was an insoluble, amorphous black solid. The reaction was then tried in a sealed glass tube in molten pyrazine and a crystalline product was produced. After this result, the reaction was attempted in a sealed high-pressure steel reactor vessel. This reaction yielded a crystalline sample with reasonable conductance. The conductivity of the sample can be calculated from the conductance by assuming that the solid obeys Ohm's law, and that the resistance at the electrodes is negligible. These assumptions are very large ones, but allow for an approximation of the conductivity in order to compare with current semiconductors. These calculations are based on the Equations 1.6 and 1.7 and the measurement of the conductance using a pressed pellet conductance setup, which is shown schematically in Figure 1.6. G is the conductance, I is the current measured, V(V) is the potential applied across the electrodes, A is the area of the electrodes, Vol($cm^3$) is the volume of

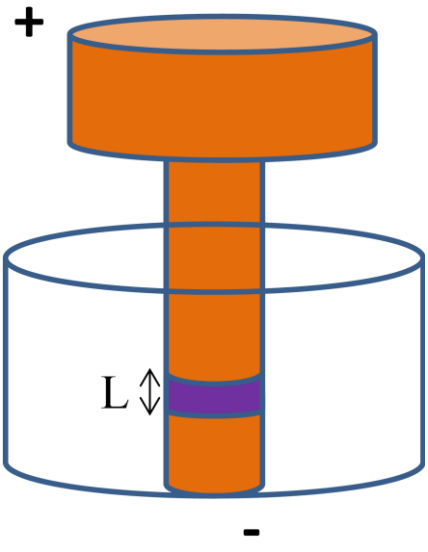


**Figure 1.6:** Conductance measurement apparatus.

the sample, L is the length of the sample, and σ is the conductivity. These equations require knowing the area of the electrodes, which can be measured, and the length of the sample, which

$$G = \frac{I}{V} = \sigma\frac{A}{L} = \sigma\frac{A^2}{Vol} \quad \text{Eqn. 1.6}$$

$$\sigma = \frac{I(A)\cdot Vol(cm^3)}{V(V)\cdot A(cm^2)^2} \quad \text{Eqn. 1.7}$$

can be calculated from the density of the sample, the mass of the sample measured, and the area of the electrodes. In order to confirm that the product was not due to one of the precursors alone, the reaction of $RuCl_2(pyz)_4$, and the reaction of $[RuCl_2(pyz)_4][BF_4]$, each in pyrazine under the same conditions was conducted, with neither yielding as crystalline of a sample, but with both yielding a low diffraction pattern which resembled the product of the two. The reaction of $[RuCl_2(pyz)_4][BF_4]$ with itself also showed a reduced conductance, pointing towards the fact that the reaction is optimized when both ruthenium(II) and ruthenium(III) are present. This can be attributed to the fact that the ruthenium(II) or ruthenium(III) compounds alone can still form the same network, but will not be mixed-valence, so will have reduced conductance. The optimal sample of the reaction of $RuCl_2(pyz)_4$ and $[RuCl_2(pyz)_4][BF_4]$ has been sent to Brookhaven National Labs, to a collaborator, to be analyzed under synchrotron radiation, and hopefully the structure can then be solved. All data for ruthenium networks is compared in Table 1.1.

Also underway is the reaction of ruthenium(II)hexa(acetonitrile)-tetrafluoroborate with

$$[Ru(NCCH_3)_6][BF_4]_2 + [RuCl_2(pyz)_4][BF_4] \rightarrow [Ru(pyz)_6RuCl_2][BF_4]_3 \quad \text{Eqn. 1.8}$$

ruthenium(III)tetra(pyrazine)dichloride-tetrafluoroborate. The synthesis of $[Ru(NCCH_3)_6][BF_4]_2$ is a novel route, and could allow for interesting mixed-valence coordination frameworks, even

though the coordination of the ruthenium metal centers would not be homogeneous, which could cause localization of mixed-valence states.

*Cobalt pyrazine networks*

The synthesis of $[CoCl_2(pyr)_4][Cl]$ was reported in the literature.[16] An aqueous exchange of chloride anion for hexafluorophosphate was performed, and confirmed by solubility tests, UV-Vis spectroscopy, and $^1$H-NMR. $[CoCl_2(pyr)_4][PF_6]$ was then reacted under multiple different conditions to yield the tetra(pyrazine) substituted product, but all reactions yielded an insoluble product.

The direct synthesis of a cobalt(III)tetra(pyrazine) precursor was then attempted. Cobalt(II)chloride was combined with pyrazine in solution, and chlorine gas and silver salts with non-coordinating anions such as tetrafluoroborate, trifluoromethanesulfonate (triflate), and hexafluoroantimonate were added. This is shown in Scheme 1.2. The reaction with silver tetrafluoroborate yielded a green solid, as would be expected for a cobalt(III) complex, but the product had almost no solubility. The reaction with silver triflate yielded an insoluble tan solid, and the reaction with hexafluoroantimonate showed no reaction at all. The reaction of cobalt(II)bromide with pyrazine, bromine, and silver tetrafluoroborate was also attempted, but yielded no reaction. A soluble cobalt(III) tetra(pyrazine)-substituted precursor could not be synthesized, so the project was abandoned.

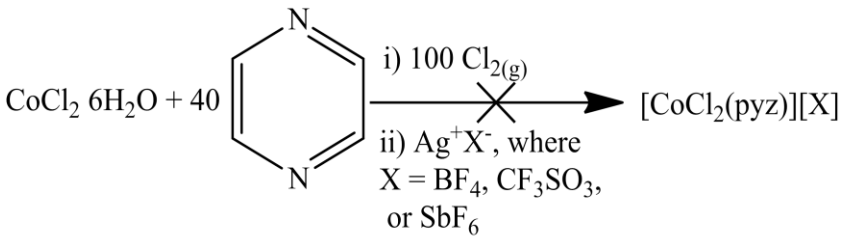


**Scheme 1.2:** Reaction of cobalt(II)chloride with pyrazine, chlorine, and silver salts.

**Conclusions**

The formation of extended solid analogs of the Creutz-Taube reaction is of interest for solution-processable semiconductors. The reaction of mixed-valence precursors under correct experimental conditions has yielded compounds whose properties are currently under investigation. More work is necessary in order to optimize the synthesis of a crystalline semiconducting product.

More work is also required for the reaction of $[Ru(NCCH_3)_6][BF_4]$ with other ruthenium precursors. This work, while not originally intended, could prove to be interesting for the study of electron-transfer through the extended solid, and also as a comparison between mixed-valence frameworks in which all of the metal centers are either the same or variable.

The synthesis of mixed-valence cobalt pyrazine precursors is required in order for this work to proceed, but is worth the effort due to the comparison between the ruthenium and cobalt networks that would be possible. Since cobalt metal centers have significant changes in properties when changing from cobalt(II) to cobalt(III), the mixed-valence framework would be enlightening.

**Experimental**

**Physical Measurements.** UV-Vis spectra were obtained using a JASCO V-530 photometer running Spectra Manager for Windows 95/NT version 1.50.00. FT-IR spectra were obtained using a JASCO FT/IR-4100 running Spectra Manager version 2.05.02. $^1$H-NMR were obtained using either a Bruker AVANCE/500 or Bruker AVANCE/360 spectrophotometer running Bruker Topspin version 1.3 and interpreted using MestReC version 4.9.9.9. The chemical shift values were internally referenced to deuterated solvent residual resonances. Room-temperature solid state conductivity was obtained using a Princeton Applied Research EG&G Potentiostat/Galvanostat model 263A running CorrWare for Windows 95/NT 32-bit

version 2.2, with the samples contained in a lab-built apparatus that consists of a Delrin block with a 6.35 mm cylindrical hole and two 6.35 mm cylindrical copper contacts. The material to be measured was deposited between the two contacts and compressed with a 3.85 kg weight on the top contact, in a two-electrode configuration. Preliminary powder x-ray diffraction data was obtained using a Bruker D2 phaser running DiffracSuite version 1.0.7 using Cu-Kα radiation. Powder x-ray diffraction data was interpreted using Bruker AXS software TOPAS version 4.2 and EVA version 15.0.0.0.

**Reaction apparatus.** Photolysis was performed in a Rayonet photochemical reactor model RPR-100, using UV bulbs model RPR-3500A. All oxygen or moisture sensitive reactions were performed using standard Schlenk line techniques. High-pressure, high-temperature pressure vessel reactors were purchased from Parr Instruments.

**Materials.** All solvents were obtained from commercial suppliers and used as received except as noted below. Dry acetonitrile was prepared by refluxing acetonitrile over $P_2O_5$ and stored over 3 Å sieves under vacuum until used. Dry dichloromethane was prepared by refluxing dichloromethane over $P_2O_5$ and stored over $CaH_2$ under vacuum until used. Dry heptane was prepared by refluxing over Na and stored over sodium benzoquinone under vacuum until used. $RuCl_2(DMSO)_4$ **(1)**,[17] $RuCl_2(pyz)_4$ **(2)**,[18] $RuCl_2(NCCH_3)_4$ **(3)**,[19] tris(p-bromophenyl)amine,[20] and $[CoCl_2(pyr)_4][Cl]$[16] were synthesized by previous literature procedures.

*Ruthenium pyrazine networks*

**$RuCl_2(pyz)_4$.** $^1$H NMR ($CD_3CN$): δ 8.44 (d, 8H), 8.33 (d, 8H).

**Tris(p-bromophenyl)amine.** $^1$H NMR ($CDCl_3$): δ 7.37-7.33 (m, 6H), 6.94-6.90 (m, 6H).

**$[Ru(NCCH_3)_6][BF_4]_2$ (4).** $RuCl_2(NCCH_3)_4$ (221.0 mg, 0.6574 mmol) and $AgBF_4$(311.3 mg, 1.599 mmol) were dissolved under nitrogen atmosphere in dry acetonitrile (10.0 mL) and shielded from light. The solution was refluxed for 5 days, cooled, and filtered in air to isolate AgCl (165.1 mg, 88% theoretical yield). The product was then precipitated with $Et_2O$ (10.0 mL) and filtered to isolate shiny white solid. The product was tested for $AgBF_4$ content by dissolving in minimal amount of water and adding aqueous NaCl solution to show that no AgCl precipitated from solution. Yield of $[Ru(NCCH_3)_6][BF_4]_2$: 263.9 mg, 77%. $^1$H NMR ($D_2O$): δ 2.53 (s, 18H).

**Tris(p-bromophenyl)ammoniumyl tetrafluoroborate.** $NOBF_4$ (145 mg, 1.24 mmol) was dissolved in the dark in ~50 mL dry acetonitrile under nitrogen atmosphere. The solution was treated with tris(p-bromophenyl)amine (605 mg, 1.25mmol). The solution immediately turned blue. The solution was stirred for 1 hour under nitrogen atmosphere. After stirring at room temperature, the solution was exposed to active vacuum until ~5 mL of solvent was removed in order to remove nitric oxide, in order to force reaction equilibrium as far as possible. The solution was filtered and the solvents were removed under vacuum. The filtered residue was dissolved in dry $CH_2Cl_2$ (~50 mL). Dry heptane (~30 mL) was vacuum transferred onto solution, the solution was warmed to room temperature, and the volume was slowly reduced to ~45 mL under vacuum to recrystallize the product. The solution was filtered to isolate the blue crystalline product. Yield of $[(BrC_6H_4)_3N][BF_4]$: 430 mg, 61%. UV-Vis $\lambda_{max}$=740 nm(22,800 ε).

**$[RuCl_2(pyz)_4][BF_4]$ (5).** $RuCl_2(pyz)_4$ (200.3 mg, 0.4068 mmol) and pyrazine(70.0 mg, 0.874 mmol) were dissolved under nitrogen atmosphere in dry $CH_2Cl_2$ (~200 mL) in dark. The solution was filtered under nitrogen atmosphere to isolate homogeneous solution, and dry solution of tris(p-bromophenyl)ammoniumyl tetrafluorborate (235 mg, 0.411 mmol) in $CH_2Cl_2$ (~30 mL) was added under nitrogen counterflow. Stirring in the dark for 1.5 hours produced a

gold precipitate. Reduction of volume to half of total volume, and subsequent filtering under nitrogen yielded the product as a shiny gold powder. Yield of $[RuCl_2(pyz)_4][BF_4]$: 153.4 mg, 65%.

*Cobalt pyrazine mixed-valence materials*

**$[CoCl_2(pyr)_4][PF_6]$.** $[CoCl_2(pyr)_4][Cl]$ (1.0324 mg, 2.1433 mmol) was dissolved in $H_2O$ (250 mL). To this solution, a saturated aqueous solution of $KPF_6$ (0.5079 g, 2.759 mmol, 10 mL) was added. Immediately, a light green precipitate formed. This light green precipitate was washed with water and diethyl ether. Yield of $[CoCl_2(pyr)_4][PF_6]$: 968.8 mg, 76%. $^1H$ NMR($CDCl_3$): δ 8.42 (d, 2H), 8.02 (t, 1H), 7.38 (t, 2H).

**Table 1.1:** Reactions to form Extended Solids

| Reactants | Solvent | Temperature & Duration | Crystallinity | Conductance (A/V) 10 mg | Color | Expected Structural Formula | Yield *** |
|---|---|---|---|---|---|---|---|
| 1,5 | MeCN | 75 °C, 24 hr | Amorphous | $3.7x10^{-7}$ | Black | $\{[Ru_2Cl_4(pyz)_4][BF_4]\}$ | 66 % |
| 1,5 | MeCN | hν, 2 hr | Amorphous | Non-conducting | Light tan | $\{[Ru_2Cl_4(pyz)_4][BF_4]\}$ | 79 % |
| 3,5 | MeCN | 87 °C, 24 hr | N/A | N/A | Dark red solution | $\{[Ru_2Cl_4(pyz)_4][BF_4]\}$ | N/A |
| 2, 5 | MeCN | RT, 2 days | N/A | N/A | Light red solution | $\{[Ru_2Cl_4(pyz)_4][BF_4]\}$ | N/A |
| 2,5, pyz | MeCN | 135 °C, 36 hr | Amorphous | Non-conducting | Black | $\{[Ru_2Cl_4(pyz)_4][BF_4]\}$ | 93 % |
| 2,5, pyz | DMAC | 135 °C, 3 days | Amorphous | $0.2x10^{-7}$ | Black | $\{[Ru_2Cl_4(pyz)_4][BF_4]\}$ | 100 % |
| 2,5 | pyz | 70 °C, 7 days | +a | N/M | Dark red and black | $\{[Ru_2Cl_4(pyz)_4][BF_4]\}$ | 207 % |
| 2,5 | pyz | 135 °C, 3 days | +b * | $2.2x10^{-5}$ ** | Red | $\{[Ru_2Cl_4(pyz)_4][BF_4]\}$ | 113 % |
| 2 | pyz | 135 °C, 24 hr | +c | N/M | Red | $\{[Ru_2Cl_4(pyz)_4][BF_4]\}$ | 147 % |
| 5 | pyz | 135 °C, 24 hr | +d | $1.0x10^{-7}$ | Red | $\{[Ru_2Cl_4(pyz)_4][BF_4]\}$ | 131 % |
| 4 | pyz | 135 °C, 3 days | +e | N/M | Orange | $\{[Ru(pyz)_3][BF_4]_2\}$ | 72 % |
| 4, pyz | MeCN | 87 °C, 3 days | N/A | N/A | Light tan solution | $\{[Ru(pyz)_3][BF_4]_2\}$ | N/A |
| 4,5 | pyz | 135 °C, 5 days | +f | N/M | Red | $\{[Ru(pyz)_4RuCl_2][BF_4]_3\}$ | 149 % |

+ See Figure 1.6 and Chart 1.1 for comparison of crystallinity. N/A = not applicable

* Sample is currently being studied at Brookhaven in order to determine structure. N/M = not measured

** Conductance measurements of potential soak at 1V and -1V shown in Figure1.7.

*** Yield is based on the assumption that the product matches the expected formula shown.

**Figure 1.7:** Powder Diffraction Patterns of Ruthenium Networks

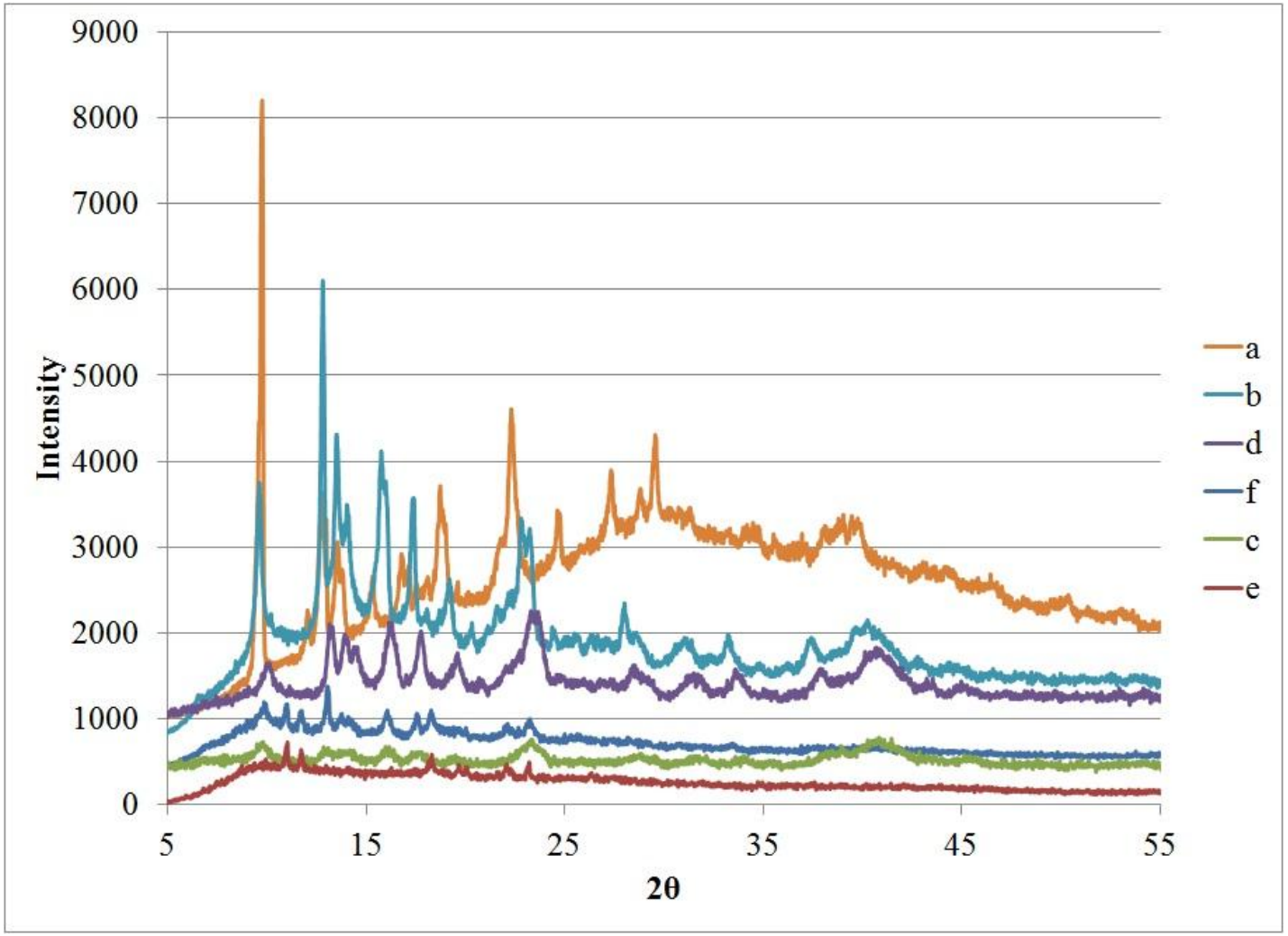


See Table 1.1 for reaction conditions.

**Chart 1.1:** Peak Assignments for Crystalline Ruthenium Networks

| Compound | Pseudo Voit Peak Position (2θ) (d-spacing(Å)) | | | | | | | | | | | | | | | | | | |
|---|---|---|---|---|---|---|---|---|---|---|---|---|---|---|---|---|---|---|---|
| a | 9.73 (9.09) | 12.07 (7.33) | 12.78 (6.92) | 13.56 (6.53) | 13.83 (6.40) | 15.30 (5.79) | 16.86 (5.26) | 17.87 (4.96) | 18.80 (4.72) | 21.73 (4.09) | 22.34 (3.98) | 24.67 (3.61) | | 27.32 (3.26) | 28.75 (3.10) | 29.55 (3.02) | | | |
| b | 9.64 (9.17) | | 12.82 (6.90) | 13.53 (6.54) | 14.05 (6.30) | | 15.83 (5.59) | 17.35 (5.11) | 19.15 (4.63) | 20.30 (4.37) | 22.86 (3.89) | 23.26 (3.82) | | 27.99 (3.18) | 28.65 (3.11) | 31.04 (2.88) | 33.22 (2.69) | 37.38 (2.40) | 40.21 (2.24) |
| c | 9.77 (9.05) | | 12.95 (6.83) | 13.96 (6.34) | | | 16.09 (5.50) | 17.63 (5.03) | | | | 23.27 (3.82) | | | 28.72 (3.11) | 31.69 (2.82) | 33.92 (2.64) | 38.44 (2.34) | 40.78 (2.21) |
| d | 10.06 (8.79) | | | 13.24 (6.68) | 13.94 (6.35) | 14.48 (6.11) | 16.23 (5.46) | 17.75 (4.99) | 19.54 (4.54) | | | 23.25 (3.82) | 23.69 (3.75) | | 28.64 (3.11) | 31.50 (2.84) | 33.68 (2.66) | 37.87 (2.37) | 40.73 (2.21) |
| e | | 10.99 (8.04) | 11.75 (7.53) | | | | | 18.28 (4.85) | 19.67 (4.51) | 20.06 (4.42) | 22.12 (4.02) | 23.17 (3.84) | | | | | | | |
| f | 9.72 (9.10) | 11.00 (8.04) | 11.74 (7.53) | 13.06 (6.77) | 13.95 (6.34) | 16.06 (6.51) | 17.56 (5.05) | 18.29 (4.85) | | | 22.16 (4.01) | 23.22 (3.83) | | | | | | | |

See Table 1.1 for reaction conditions.

**Figure 1.8:** Conductance Measurements at 1 V and -1 V Potential Soak for Compound b.

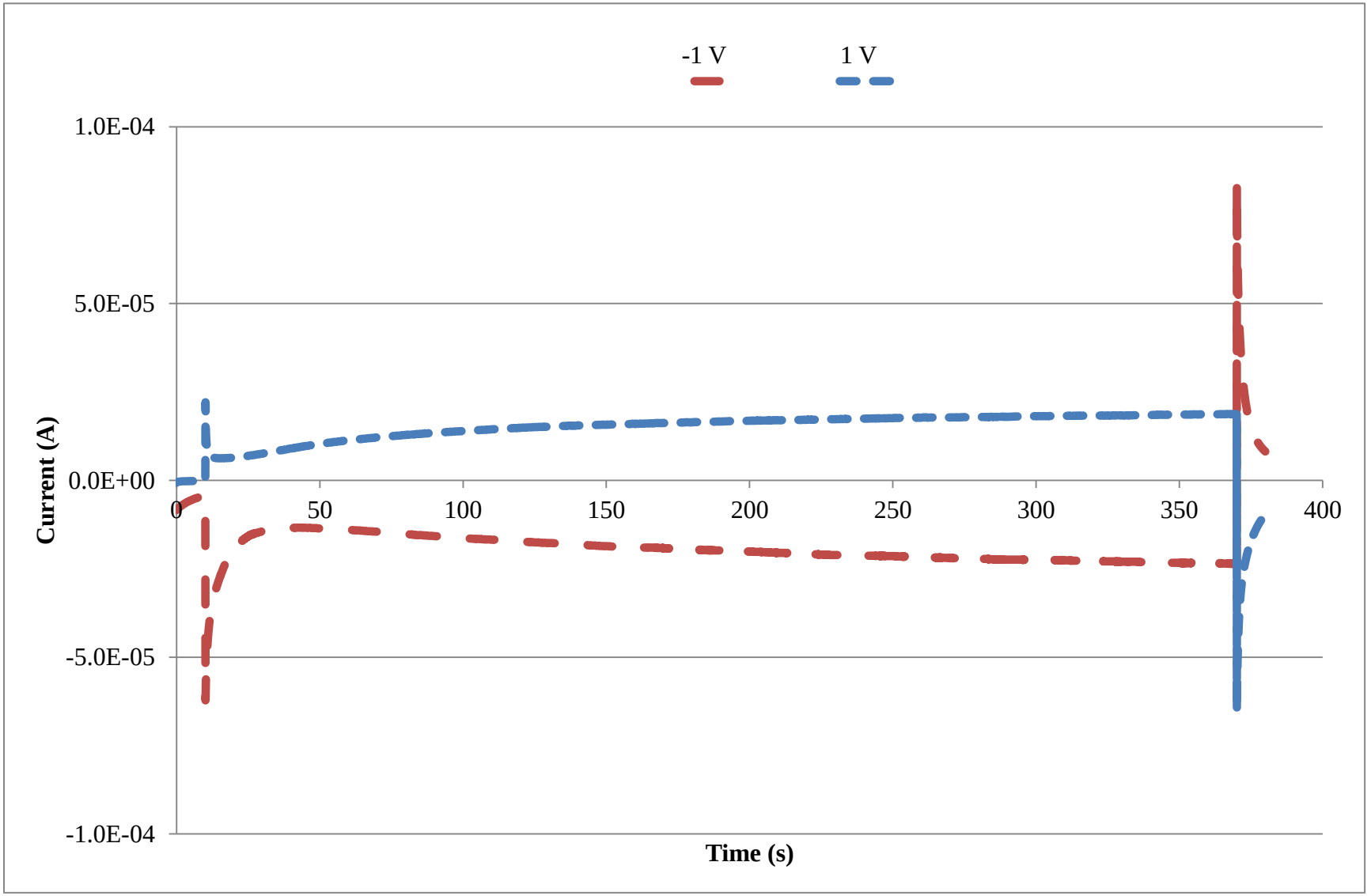

## References


[1] Janata, J. *Principles of Chemical Sensors*, 2nd Edition; Springer Science+Business Media: New York, 2009.

[2] Tranchemontagne, D. J.; Mendoza-Cortes, J. L.; O'Keeffe, M.; Yaghi, O. M. *Chem. Soc. Rev.* **2009**, *38*, 1257-1283.

[3] Robin, M. B.; Day P. *Advances in Inorganic Chemistry and Radiochemistry*. **1967**, *10*, 237-422.

[4] Marcus, R. A. *J. Chem. Phys.* **1956**, *24*, 966-978.

[5] Marcus, R. A. *Electrochim. Acta.* **1968**, *13*, 995-1004.

[6] Hush, N. S. *J. Chem. Phys*. **1958**, *28*, 962-972.

[7] Hush, N. S. *Electrochim. Acta.* **1968**, *13*, 1005-1023.

[8] Taube, H. *Electron Transfer Reactions of Complex Ions in Solution*; Current Chemical Concepts; Academic Press, Inc: New York, NY,1970.

[9] Brunschwig, B. S.; Creutz, C.; Sutin, N. *Chem. Soc. Rev.* **2002**, *31*, 168-184.

[10] Demadis, K. D.; Hartshorn, C. M.; Meyer, T. J. *Chem. Rev.* **2001**, *101*, 2655-2685.

[11] Creutz, C.; Taube, H. J. *J. Am. Chem. Soc.* **1969**, *9*, 1, 3988-3989.

[12] von Kameke, A.; Tom, G. M.; Taube, H. *Inorg. Chem.* **1978**, *17*, 1790-1796.

[13] Elgy, C. N.; Wells, C. F. *J. Chem. Soc., Dalton Trans*. **1980**, No. 12, 2405-2409.

[14] Duliere, E.; Devillers, M.; Marchand-Brynaert, J. *Organometallics*. **2003**, *22* (4), 804-811.

[15] Carlucci, L.; Ciani, G.; Porta, F.; Proserpio, D. M.; Santagostini, L. *Angew. Chem., Int. Ed*. **2002**, *41* (11), 1907-1911.

[16] Brindell, M.; Stochel, G.; Bertolasi, V.; Boaretto, R.; Sostero, S. *Eur. J. Inorg. Chem*. **2007**, No. 16, 2353-2359.

[17] Baker, T. N.; Doherty, W. P., Jr.; Kelley, W. S.; Newmeyer, W.; Rogers, J. E., Jr.; Spalding, R. E.; Walter, R. I. *J. Org. Chem*. **1965**, *30* (11), 3714-3718.

[18] Barton, D. H. R.; Haynes, R. K.; Leclerc, G.; Magnus, P. D.; Menzies, I. D. *J. Chem. Soc., Perkin Trans. 1*. **1975**, No. 20, 2055-2065.

[19] Jahn, U.; Aussieker, S. *Org. Lett*. **1999**, *1*(6), 849-852.

[20] Lever, A. B. P. *Inorg. Chem*. **1990**, *29*(6), 1271-1285.

# CHAPTER 2

# METAL ORGANIC FRAMEWORKS

## Introduction

Metal organic frameworks, in comparison to CFs, are bound covalently between the metal centers and the organic spacers. MOFs should, therefore, have higher electronic communication between the metal center and the organic spacer. One effect of this increased communication is that organic spacers which possess electron delocalization across the entire molecule will cause higher electronic communication throughout the framework. Another effect of the covalent bonds is that the frameworks should be more stable chemically and thermally than frameworks connected by dative bonds. This can be both a positive and a negative property due to the fact that the enhanced stability could allow for more applications, but the formation of the networks will require a reversible synthetic pathway to increase the crystallinity of frameworks formed.

A third effect is that the HOMO-LUMO gap will have a direct effect on the band gap of the extended solid. This is due to the fact that an unfilled molecular orbital lying close to the filled metal atomic orbitals can allow for the electron transfer to occur between metal centers and organic spacers. This process would rely on the thermal energy at room temperature to surmount the activation energy for electron transfer.

Metal organic frameworks synthesized using thiolate multidentate ligands have been shown to produce extended solids with reasonable conductivities.[1] These solids were crystalline, dopable, and air-stable. This is to be expected by considering thiolate frameworks as analogs of

current inorganic semiconductors. The small band gap semiconductor PbS ($E_g \approx 0.4$ eV) is analogous to the compound $[Pb(SC_6H_4S)]_n$, if one considers 1,4-benzenedithiol to be analogous to $H_2S$. Also, considering that another inorganic semiconductor titanium dioxide, or $TiO_2$, is analogous in the same way to $[Ti(OC_6H_4O)_2]_n$, then using sulfur- or selenium-containing analog instead of an oxygen-containing organic spacer would lessen the band gap due to lower atomic orbitals, resulting in lower molecular orbitals, and improve the conductivity of the material. By using organic ligands which have lower lying LUMOs, the conductivity of MOFs synthesized from thiolate ligands should be improved. Towards this end, an anthracene-based tetrathiol with protecting groups has been synthesized.

In a related project, attempts have been made to synthesize benzene-based selenolate ligands and to form frameworks based on these ligands as isostructural analogues of current thiolate frameworks.

Another project has also begun where MOFs in the literature are synthesized and then attempts are made to impregnate them with non-coordinating ions and form a mixed-valence MOF. Towards this end, a MOF was selected which has large pore sizes so that guest solvents could be removed and replaced with tetrafluoroborate anions. This project has not shown appreciable results.

**Results and Discussion**

***Anthracene Thiolate Frameworks***

The complete synthesis of 9,10-dimethyl-2,3,6,7-tetra(((1-methyl-4-pyridin-1-iumyl)ethyl)thio)-anthracene tetra(tetrafluoroborate) (**$(Me)_4\mathbf{1}^{4+}[BF_4]_4$**) is shown in Scheme 2.1. This route was chosen in order to afford a protected anthracene-based polythiol in which the leaving group could be easily removed, and the polythiol could be generated in-situ.

The reaction of dimethoxybenzene and various aldehydes in order to yield substituted anthracenes has been published in the literature.[2,3] The reaction of 2,3,6,7-tetramethoxy-9,10-

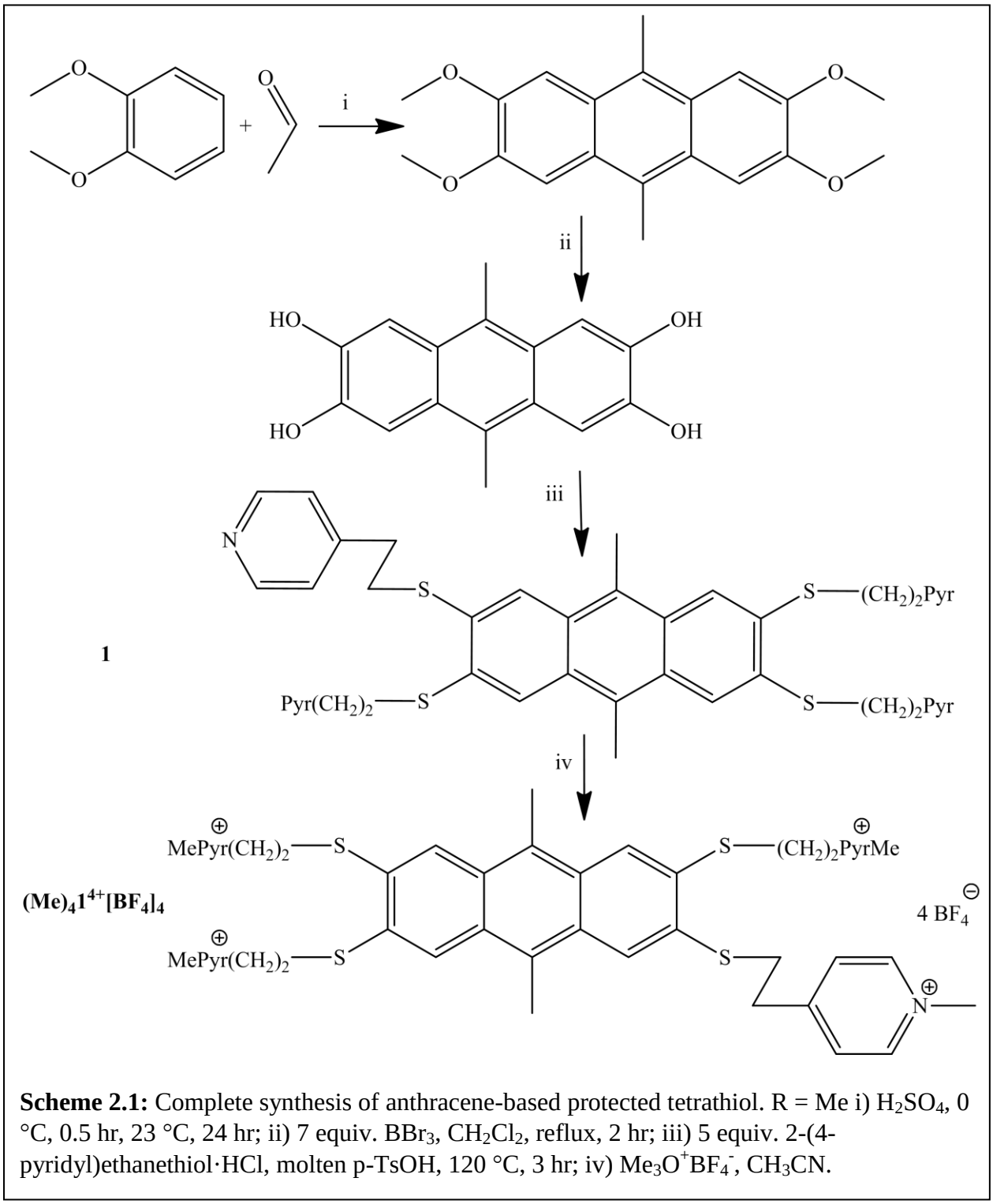


1

**(Me)$_4$1$^{4+}$[BF$_4$]$_4$**

**Scheme 2.1:** Complete synthesis of anthracene-based protected tetrathiol. R = Me i) $H_2SO_4$, 0 °C, 0.5 hr, 23 °C, 24 hr; ii) 7 equiv. $BBr_3$, $CH_2Cl_2$, reflux, 2 hr; iii) 5 equiv. 2-(4-pyridyl)ethanethiol·HCl, molten p-TsOH, 120 °C, 3 hr; iv) $Me_3O^+BF_4^-$, $CH_3CN$.

dimethylanthracene with 7 equivalents of boron tribromide yielded the tetrahydroxyanthracene with ½ an equivalent of diethyl ether as a solvent of crystallization in a very good yield.

There was evidence in the literature that mercaptoethylpyridine·HCl could provide a good thiol source, and that the pyridine ring could then be methylated and the protecting group removed.[4] 2,3,6,7-tetrahydroxy-9,10-dimethylanthracene·1/2 diethyl ether was treated with mercaptoethylpyridine·HCl in p-toluenesulfonic acid at 120 °C for three hours under a nitrogen atmosphere, applying vacuum every 15 minutes in order to remove water produced in reaction. The reaction mixture was worked up with aqueous $NaHCO_3$, extracted with dichloromethane, dried via rotary evaporation, and the resulting solid was recrystallized from acetone to yield pure 9,10-dimethyl-2,3,6,7-tetra(((4-pyridinyl)ethyl)thio)-anthracene (**1**).

The methylation route in the literature was to use MeI and then immediately deprotect with mildly basic conditions, followed by protonation of the thiol with acid. The methylation was performed at first as suggested, where **1** was dissolved in dry acetonitrile and reacted with iodomethane under nitrogen atmosphere. This solution was refluxed for 4.5 hours, and during the course of the reflux the solution became homogeneous. The product, 9,10-dimethyl-2,3,6,7-tetra(((1-methyl-4-pyridin-1-iumyl)ethyl)thio)-anthracene tetraiodide·2/3 diethyl ether (**$(Me)_4\mathbf{1}^{4+}[I]_4$**), was isolated by precipitation with diethyl ether. The $^1$H NMR of the sample had a large water peak which obscured one of the methylene proton peaks from the protecting group and the methylene peak from the ether. **$(Me)_4\mathbf{1}^{4+}[I]_4$** was then reacted with acetic anhydride in DMF with $K_2CO_3$ as the deprotecting base, DMF with TEA, and acetonitrile with TEA. None of these reactions produced the tetra-acetyl protected thiol as a pure product, so the decision was made to attempt to work with the tetrafluoroborate-containing product, **$(Me)_4\mathbf{1}^{4+}[BF_4]_4$**, to make the MOFs and remove the pyridiniumyl protecting group during the reaction with the metal salts.

**1** was then reacted with trimethyloxonium tetrafluoroborate under static vacuum in dry acetonitrile in order to methylate the pyridine rings. The product of this reaction was precipitated out of solution with diethyl ether and characterized by $^{1}H$ NMR. The $^{1}H$ NMR showed pure product.

Equation 2.1 shows the intended reaction with lead(II) acetate. In order to achieve this, **$(Me)_4\mathbf{1}^{4+}[BF_4]_4$** was reacted with two equivalents of lead(II) acetate in ethylenediamine.

$$[C_{16}H_{10}(SCH_2CH_2PyrMe)_4][BF_4]_4 + 2\ Pb(OAc)_2{\cdot}3H_2O \rightarrow \qquad \text{Eqn. 2.1}$$

$$[Pb(S_2C_{16}H_{10}S_2)Pb]$$

The ethylenediamine appeared to be causing a reaction with **$(Me)_4\mathbf{1}^{4+}[BF_4]_4$** before addition of the lead salt. This could be attributed to the deprotection of the thiol functionalities, so the lead solution was added and the reaction mixture was heated to 60 °C and held at steady temperature for 16 hours. A yellow solid precipitated out of solution, and upon exposure to air, the solid turned green. Powder x-ray diffraction revealed that the solid was amorphous, so a different solvent for the reaction was decided upon.

**$(Me)_4\mathbf{1}^{4+}[BF_4]_4$** was soluble in DMF and lead(II) acetate was soluble in methanol, so the two separate solutions were made up. These two solutions were combined at room temperature and no reaction seemed to occur. The combined solution was heated to 60 °C and held at steady temperature for 16 hours, at which time significant amounts of orange solid had precipitated out. The solid was isolated, washed with diethyl ether, and a powder diffraction of the solid was measured. During the course of the powder diffraction, the orange solid darkens appreciably. The powder diffraction revealed that this product was also amorphous.

After the unsuccessful synthesis of crystalline extended solids based on protected tetrathiolanthracene, another avenue was investigated. Equation 2.2 shows the intended reaction.

$$[C_{16}H_{10}(SCH_2CH_2PyrMe)_4][BF_4]_4 + 2\ Ni\ (OAc)_2\cdot 4H_2O + xs\ TMEDA \rightarrow \quad \text{Eqn. 2.2}$$

$$[(C_6H_{16}N_2)Ni(S_2C_{16}H_{10}S_2)Ni(C_6H_{16}N_2)]$$

**$(Me)_4\mathbf{1}^{4+}[BF_4]_4$** was reacted with two equivalents of nickel(II) acetate in dry DMF, and then treated with excess TMEDA in order to precipitate out a black solid. The solid was washed with methanol and diethyl ether, then powder x-ray diffraction and room temperature pressed pellet conductivity of sample were measured. The solid was amorphous but showed some conductance, on the order of $2x10^{-5}$ A/V for 10 mg of sample. The sample was tested for solubility in an attempt to recrystallize, but was completely insoluble. If the intended product was synthesized, then the reaction with tetra(ethyl)ethylenediamine, or a longer alkyl substituted ethylenediamine should increase solubility. The other future work for this project is to synthesize anthracene precursors which contain longer alkyl chains at the 9 and 10 positions in order to increase solubility.

*Benzene Selenolate Frameworks*

In order to synthesize analogous frameworks to current frameworks in the literature, selenium has been substituted for sulfur on existing thiolate MOF spacers and the MOF syntheses attempted. This requires the synthesis of *t*-butyl-selenol substituted benzene. The first attempt made was to synthesize 1,2-bis(*tert*-butylseleno)benzene. Difluorobenzene was reacted with $LiSe^tBu\cdot$(dioxane) to yield a yellow oil. $^1H$ NMR was very convoluted and contained many impurities, even after silica gel chromatography, so the sample was submitted for analysis by mass spectrometry. Dr. Qiaoli Liang conducted EI mass spectrometry of the sample, along with APCI-MS and high resolution MS. It was determined that only one fluorine on the benzene had been substituted by selenium and that a diselenide bridge between two mono-substituted benzene compounds had formed. The next attempt was to make hexakis(*tert*-butylseleno)benzene. This

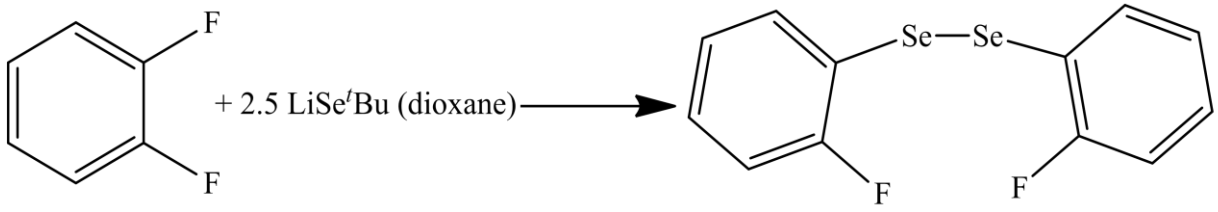


**Scheme 2.2:** Reaction of difluorobenzene with lithium *t*-butyl selenide.

compound had already been made,[5] however, hexachlorobenzene used in the synthesis is no longer available. The synthesis of hexakis(*tert*-butylseleno)benzene was performed in the same manner using hexabromobenzene, with only a slight reduction in yield.

Hexakis(*tert*-butylseleno)benzene was then treated with lead(II) acetate in ethylenediamine at reflux for 24 hours. The intended reaction is shown in Equation 2.3. This yielded an amorphous, insoluble brown powder with very low conductivity.

$$C_6(Se^tBu)_6 + 3Pb(OAc)_2 \cdot 3H_2O \rightarrow [Pb_3(C_6Se_6)] \qquad \text{Eqn. 2.3}$$

Hexakis(*tert*-butylseleno)benzene was then treated with lead(II) acetate in 2-methoxyethanol in hopes that the methoxyethanol would be less basic, and would therefore cause less side reactions. Solution of hexakis(*tert*-butylseleno)benzene and lead(II) acetate was heated to 75 °C for two hours and no reaction appeared to be occurring. In order to force a reaction, one drop of concentrated hydrochloric acid was added to the solution. There was an immediate color change from the pink color of starting hexa(seleno)benzene to a yellow color. After stirring overnight at 80 °C, significant amount of yellow solid had precipitated out of solution. This yellow solid was isolated, and its powder diffraction and conductance was measured. The solid has almost no conductivity, but some crystallinity. There were worries about the mixing of acetate and chloride ions, so the reaction was run again. In order to avoid the mixing of chloride and acetate anions, hexakis(*tert*-butylseleno)benzene was combined with lead(II) nitrate in 2-methoxyethanol and a drop of concentrated nitric acid was added. The intended reaction is

$$C_6(Se^tBu)_6 + Pb(NO_3)_2 + HNO_3 \rightarrow [Pb_3(C_6Se_6)] \quad \text{Eqn. 2.4}$$

shown in Equation 2.4. This solution was heated to 100 °C and stirred overnight to yield an orange precipitate. The solid precipitate was isolated from the reaction. Powder x-ray diffraction measurements showed that the sample was amorphous. The further exploration of the hexa-selenol compound could yield interesting results, as preliminary data suggests crystalline and semiconducting frameworks from this organic spacer may be possible.

*Imidazolate frameworks*

The synthesis of reported compounds that are extended MOFs bound by imidazolate-based organic spacers, and post-synthesis redox chemistry to form mixed-valence MOFs was another avenue which was explored. The compound $[Co(bim)_2]\cdot(DMF)(H_2O)$ (where bim = benzimidazolate) was produced based on the reported literature procedure.[6] The crystalline sample was purified by sonication in ethanol to suspend the amorphous byproducts in solution, while the crystals sink to the bottom. After purification, removal of host solvent by refluxing in acetonitrile yielded $[Co(bim)_2]\cdot(DMF)_{0.07}(CH_3CN)_{0.93}$. The use of tris(p-bromophenyl)ammoniumyl tetrafluoroborate, as described in Chapter 1, as an oxidizing agent in both dry acetonitrile and in dry dichloromethane yielded no reaction.

**Conclusions**

The results from the MOF projects are preliminary, but suggest that there is great potential in this area for synthesis of crystalline and semiconducting frameworks. The increase of solubility of the anthracene-based protected tetrathiol is necessary for further progress. The alkyl-protected selenols appear to have promise, although further work in this area is required in order to determine proper experimental conditions for the formation of crystalline frameworks. The synthesis of mixed-valence MOFs from reported literature procedures has not shown any

progress, but further study on oxidation potentials of the metal centers in these MOFs may provide insight into other approaches. Another route in which the mixed-valence MOFs could go is to attempt the same projects on different frameworks, either changing the organic spacer or metal center.

## Experimental

**Physical Measurements.** UV-Vis spectra were obtained using a JASCO V-530 photometer running Spectra Manager for Windows 95/NT version 1.50.00. UV-Vis-NIR diffuse reflectance spectra were obtained using a Shimadzu UV-3600 spectrophotometer equipped with a Harrick Praying Mantis sample holder. FT-IR spectra were obtained using a JASCO FT/IR-4100 running Spectra Manager version 2.05.02. $^{1}$H-NMR were obtained using either a Bruker AVANCE/500 or Bruker AVANCE/360 spectrophotometer running Bruker Topspin version 1.3 and interpreted using MestReC version 4.9.9.9. The chemical shift values were internally referenced to deuterated solvent residual resonances. Room-temperature solid state conductivity was obtained using a Princeton Applied Research EG&G Potentiostat/Galvanostat model 263A running CorrWare for Windows 95/NT 32-bit version 2.2, with the samples contained in a lab-built apparatus that consists of a Delrin block with a 6.35 mm cylindrical hole and two 6.35 mm cylindrical copper contacts. The material to be measured was deposited between the two contacts and compressed with a 3.85 kg weight on the top contact, in a two-electrode configuration. Preliminary powder x-ray diffraction data was obtained using a Bruker D2 phaser running DiffracSuite version 1.0.7 using Cu-Kα radiation. Powder x-ray diffraction data was interpreted using Bruker AXS software TOPAS version 4.2 and EVA version 15.0.0.0.

**Reaction apparatus.** All oxygen or moisture sensitive reactions were performed using standard Schlenk line techniques. High-pressure, high-temperature pressure vessel reactors were

purchased from Parr Instruments. Solutions were concentrated and dried using a Büchi R-114 Rotovapor with Büchi B-480 water bath and a Brookfield TC-500 refrigerated circulating bath as a cold water supply.

**Materials.** All solvents were obtained from commercial suppliers and used as received except as noted below. Dry acetonitrile was prepared by refluxing acetonitrile over $P_2O_5$ and stored over 3 Å sieves under vacuum until used. Dry dichloromethane was prepared by refluxing dichloromethane over $P_2O_5$ and stored over $CaH_2$ under vacuum until used. Dry dimethylformamide was prepared by refluxing over P2O5 and stored over 3 Å sieves under vacuum until used. Dry 1,3-dimethyl-2-imidazolidinone was prepared by refluxing over $P_2O_5$ and stored over 3 Å sieves under vacuum until used. 2,3,6,7-tetramethoxy-9,10-dimethylanthracene[2] and $LiSe^tBu\cdot$(dioxane)[5] were prepared by literature procedures.

*Anthracene Thiolate Frameworks*

**2,3,6,7-tetrahydroxy-9,10-dimethylanthracene·1/2 diethyl ether.** Tetramethoxydimethylanthracene (2.5103 g, 7.60 mmol) was dissolved in dry $CH_2Cl_2$ (~250 mL). Under nitrogen counterflow at 0 °C, $BBr_3$ (5.1 mL, 54 mmol) was added dropwise. The resulting purple-red solution was refluxed under nitrogen atmosphere for 2 hours. The solution was poured into 0.2 N HCl (630 mL), and the product was extracted with diethyl ether (2x200 mL). The organic layers were combined and washed with water, dried over anhydrous $Na_2SO_4$, and dried on Rotovap. The sample was further dried under reduced pressure to yield a light brown solid. Yield of $(C_{16}H_{14}O_4)\cdot 1/2(C_4H_{10}O)$: 2.274 g, 95%. $^1$H NMR($CD_3CN$): δ 7.14(s, 4H), 3.42(q, 2H), 2.18(s, 6H), 1.12(t, 3H).

**9,10-dimethyl-2,3,6,7-tetra(((4-pyridinyl)ethyl)thio)-anthracene.** P-toluenesulfonic acid (19.703 g, 104 mmol) was melted under vacuum. Nitrogen atmosphere was applied to the

acid and tetrahydroxydimethylanthracene (1.592 g, 5.18 mmol) was added along with 4-mercaptoethylpyridine HCl (4.570 g, 26.0 mmol). The reaction was carried out under nitrogen atmosphere at 120 °C for 3 hours with stirring, applying vacuum every 15 minutes to remove water produced in reaction. The reaction mixture was cooled to room temperature under nitrogen atmosphere. The mixture was washed with 1.0 M $NaHCO_{3(aq)}$ (200 mL) to neutralize acid. The product was extracted from the aqueous mixture with $CH_2Cl_2$ (8x250 mL) and recrystallized from acetone to yield a light gold powder. Yield of $[(NC_7H_8S)_4(C_{16}H_{10})]$: 2.4831 g, 63 %. $^1$H NMR($CDCl_3$): δ 8.53(d, 8H), 8.12(s, 4H), 7.18(d, 8H), 3.33(t, 8H), 3.04(t, 8H), 2.98(s, 6H).

**9,10-dimethyl-2,3,6,7-tetra(((1-methyl-4-pyridin-1-iumyl)ethyl)thio)-anthracene tetraiodide·2/3 diethyl ether.** **1** (303.3 mg, 0.402 mmol) was dissolved in dry acetonitrile (100 mL) under nitrogen atmosphere. Iodomethane (584.9 mg, 4.12 mmol) was syringed into solution. The solution was refluxed for 4.5 hours. A 20 mL aliquot was removed to confirm reaction was complete. Remaining solution (80 mL) was allowed to cool to room temperature and diethyl ether (80 mL) was added. Yellow precipitate forms immediately. Filtered solution and washed with diethyl ether. Yield of $[(H_3CNC_7H_8S)_4(C_{16}H_{10})][I]_4 \cdot 2/3(C_4H_{10}O)$: 267.8 mg, 49%. $^1$H NMR($D_6$-DMSO): δ 8.90(d, 8H), 8.11(d, 8H), 8.10(s, 4H), 4.27(s, 12H), 3.62(t, 8H), 3.02(s, 6H), 1.09(t, 4H).

**9,10-dimethyl-2,3,6,7-tetra(((1-methyl-4-pyridin-1-iumyl)ethyl)thio)-anthracene tetra(tetrafluoroborate).** **1** (200.4 mg, 0.265 mmol) and trimethyloxonium tetrafluoroborate(207 mg, 1.40 mmol) were dissolved in dry acetonitrile(~10 mL). The solution was stirred at room temperature for 1.5 hrs under static vacuum. Under nitrogen counterflow, diethyl ether(15 mL) was added dropwise to precipitate gold solid. Yield of

$[(H_3CNC_7H_8S)_4(C_{16}H_{10})][BF_4]_4$: 279.9 mg, 78 %. $^1$H NMR($D_6$-DMSO): δ 8.88(d, 8H), 8.10(d, 8H), 8.08(s, 4H), 4.27(s, 12H), 3.61(t, 8H), 3.34(t, 8H), 3.02(s, 6H).

*Benzene Selenolate Frameworks*

**Hexakis(*tert*-butylseleno)benzene**. $LiSe^tBu\cdot$(dioxane) (1.801 g, 7.79 mmol) and hexabromobenzene (615.0 mg, 1.12 mmol) were dissolved in dry DMI (8.0 mL). The solution was stirred under static vacuum for 17 hours. Degassed methanol (100.0 mL) was added and the resulting solution was stirred for 30 minutes at 0 °C. The solution was filtered under nitrogen atmosphere and washed with degassed methanol (15 mL). The resulting pink solid was dried under vacuum. Yield of $[C_6(Se^tBu)_6]$: 360.2 mg, 36 %. $^1$H NMR($CDCl_3$): δ 1.44(s).

## References


[1] Turner, D. L.; Vaid, T. P.; Stephens, P. W.; Stone, K. H.; DiPasquale, A. G.; Rheingold, A. L. *J. Am. Chem. Soc.* **2008**, *130*, 14-15.

[2] Muller, S.; Raltschewa, M.; Papp, M. *Ber. Dtsch. Chem. Ges. B*. **1942**, *75B*, 692-703.

[3] Shklyaev, Y. V.; Nifontov, Y. V. *Russ. Chem. Bull*. **2002**, *51*(5), 844-849.

[4] Itoh, T.; Mase, T. *J. Org. Chem*. **2006**, *71*(5), 2203-2206.

[5] Turner, D. L. Metal-Sulfur-Organic and Metal-Selenium-Organic Network Solids. Ph.D. Dissertation, Washington University, Saint Louis, MO, 2009.

[6] Park, K. S.; Ni, Z.; Cote, A. P.; Choi, J. Y.; Huang, R.; Uribe-Romo, F. J.; Chae, H. K.; O'Keeffe, M.; Yaghi, O. M. *PNAS*. **2006**, *103*(27), 10186-10191.

# CHAPTER 3

# CONCLUSIONS

The research for this thesis is divided into two different projects, coordination frameworks and metal organic frameworks. The CF project is subdivided into two different aspects, the synthesis of the extended analog of the Creutz-Taube ion and the synthesis of the analogous pyrazine-bridged cobalt framework. The synthesis of the extended analog of the Creutz-Taube ion has yielded a crystalline and semiconducting product whose structure is currently being analyzed by synchrotron x-ray diffraction. Indexing of preliminary synchrotron x-ray diffraction data has yielded a unit cell determination which lends credence to the belief that the solid is an extended one-dimensional polymer. During the course of this synthesis, a novel ruthenium(III) compound was synthesized, ruthenium(III)dichloride-tetrapyrazine tetrafluoroborate.

Attempts to duplicate the synthesis of the precursors for the analogous cobalt project have not succeeded. This may be due to the fact that the pyrazine is not as electron-donating as the pyridine ligand, which is a viable ligand as reported in the literature. The attempts to synthesize cobalt(III)dichloride-tetrapyrazine with a non-coordinating anion by ligand exchange and directly were both unsuccessful. In order for this project to be brought to fruition, it may be necessary to choose a different metal as the metal center which has less of a requirement in order to transition between oxidation states.

In the second project, metal organic frameworks were synthesized in which the organic spacers were bound to the metals centers through covalent or ionic bonds. This project can be subdivided into three different aspects. The first aspect of the project is the synthesis of thiolate frameworks. A novel anthracene-based protected tetra-thiol has been synthesized and preliminary reactions have been performed. No crystalline frameworks have been synthesized, but this is thought to be due to poor solubility of the tetrathiolate in solution. This solubility can be improved by longer alkyl chains on the 9 and 10 positions of the anthracene ring.

The second aspect of this project involves synthesis of benzene-based polyselenols, and their reaction to form compounds which are isostructural with current literature benzene-polythiolate frameworks. Towards this end, the synthesis of 1,2-di(*tert*-butylseleno)benzene was attempted. This synthesis did not yield pure product due to formation of diselenide bridges between mono-substituted intermediates. The synthesis of hexakis(*tert*-butylseleno)benzene was successful, and preliminary reactions of this compound with lead(II) salts suggest that the product under optimized conditions could yield a crystalline framework, which is expected to be semiconducting.

The third aspect of this research was to synthesize reported frameworks which are not mixed-valence or semiconducting, and then perform redox reactions with ½ an equivalent of either reducing or oxidizing agent to yield mixed-valence MOFs. The synthesis of the reported framework with appropriate pore sizes was successful, but currently, there is no success with oxidizing the metal centers.

The synthesis of extended frameworks has been achieved to a certain degree, and further characterization is necessary in order to confirm the structure.

# APPENDIX

## $^{1}$H NMR SPECTRA

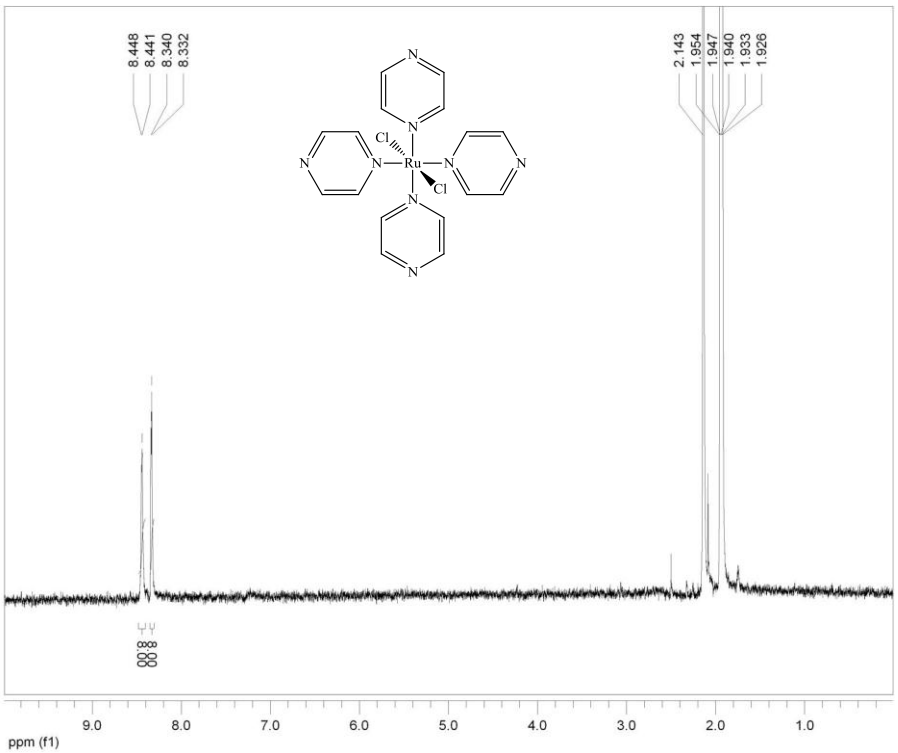
8.448
8.441
8.340
8.332
2.143
1.954
1.947
1.940
1.933
1.926
Cl
Ru
Cl
N
8.00
8.00
9.0
8.0
7.0
6.0
5.0
4.0
3.0
2.0
1.0
ppm (f1)

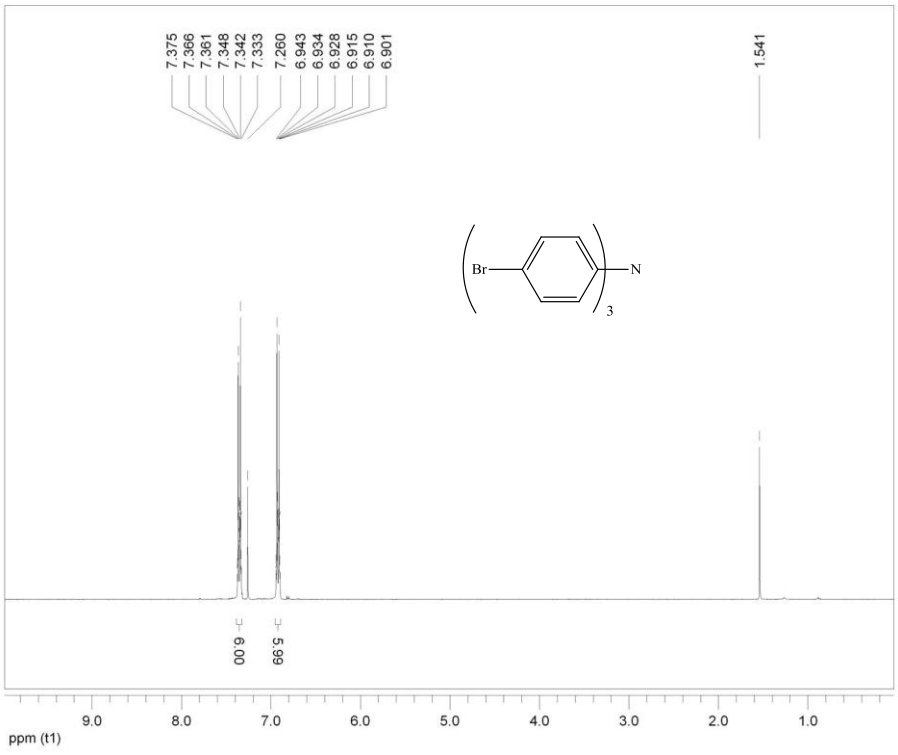
7.375
7.366
7.361
7.348
7.342
7.333
7.260
6.943
6.934
6.928
6.915
6.910
6.901
1.541
Br
N
3
6.00
5.99
9.0
8.0
7.0
6.0
5.0
4.0
3.0
2.0
1.0
ppm (t1)

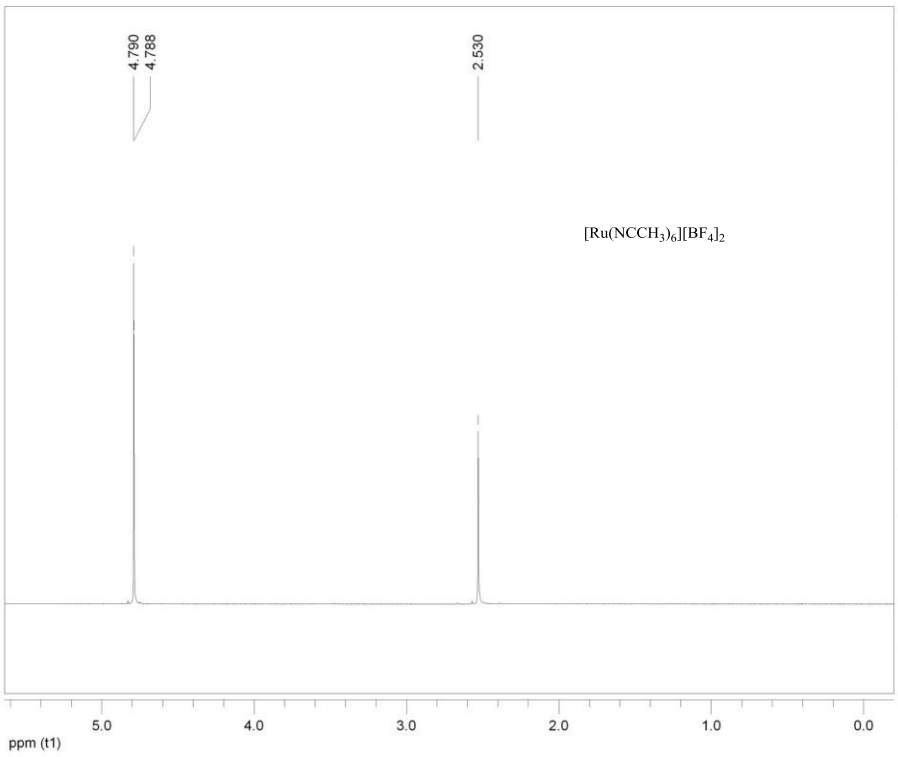
4.790
4.788
2.530
[Ru(NCCH3)6][BF4]2
5.0
4.0
3.0
2.0
1.0
0.0
ppm (t1)

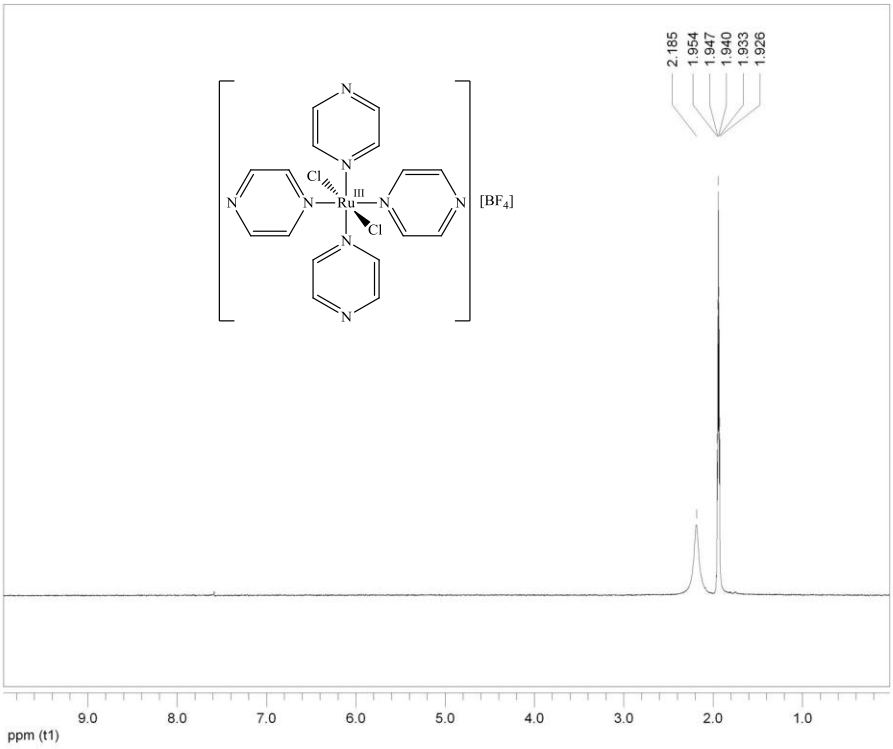
2.185
1.954
1.947
1.940
1.933
1.926
Cl
III
Ru
Cl
[BF4]
9.0
8.0
7.0
6.0
5.0
4.0
3.0
2.0
1.0
ppm (t1)

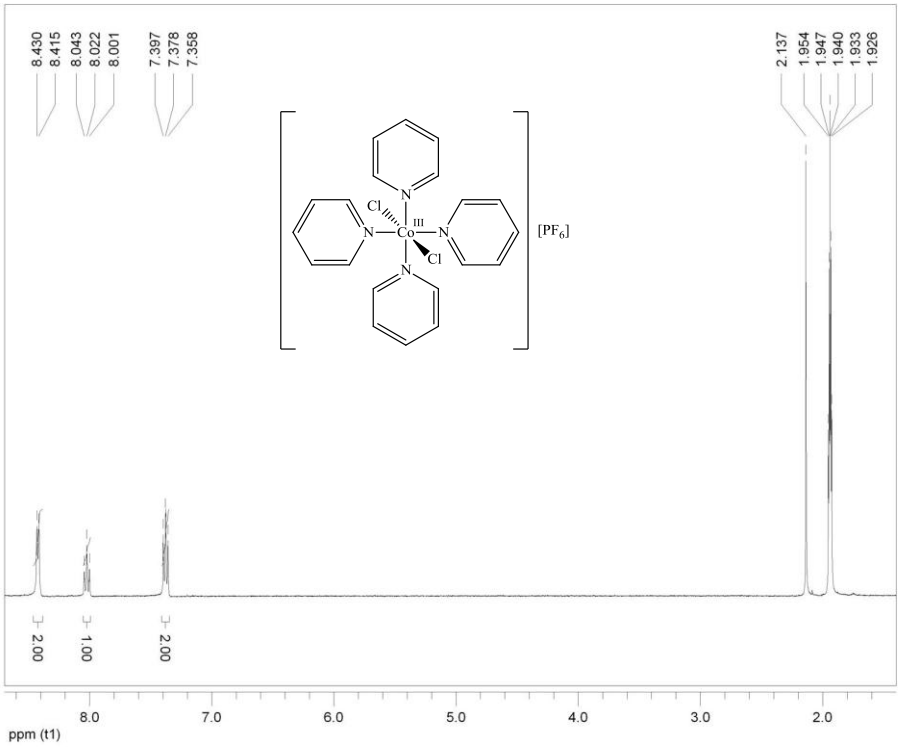
8.430
8.415
8.043
8.022
8.001
7.397
7.378
7.358
2.137
1.954
1.947
1.940
1.933
1.926
Cl
N
Co
III
N
N
Cl
N
[PF6]
2.00
1.00
2.00
8.0
7.0
6.0
5.0
4.0
3.0
2.0
ppm (t1)

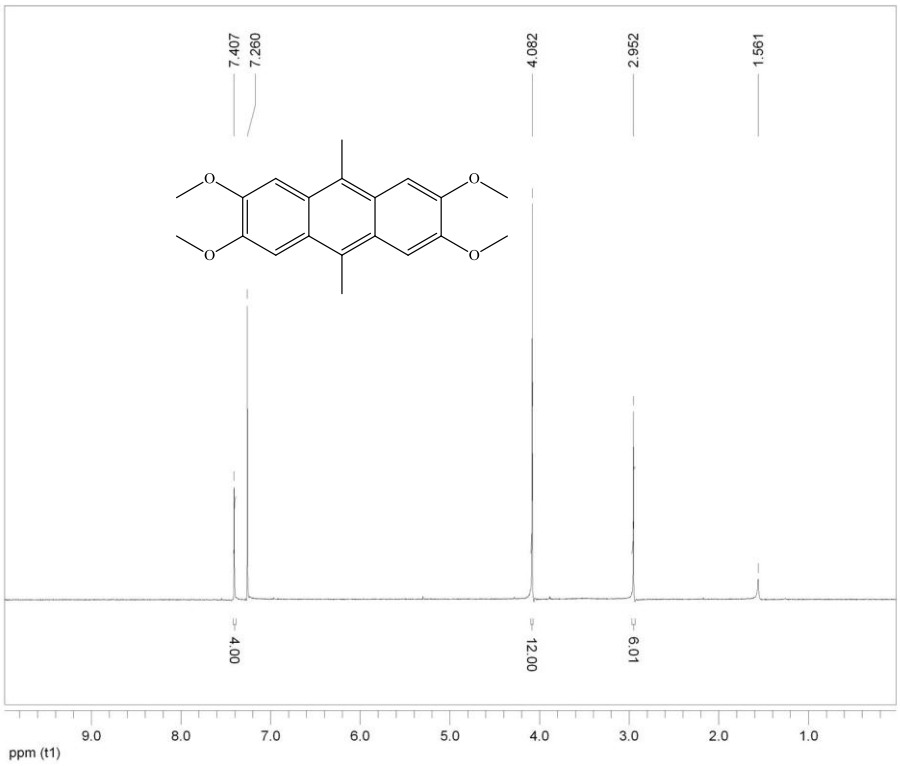
7.407
7.260
4.082
2.952
1.561
O
O
O
O
4.00
12.00
6.01
9.0
8.0
7.0
6.0
5.0
4.0
3.0
2.0
1.0
ppm (t1)

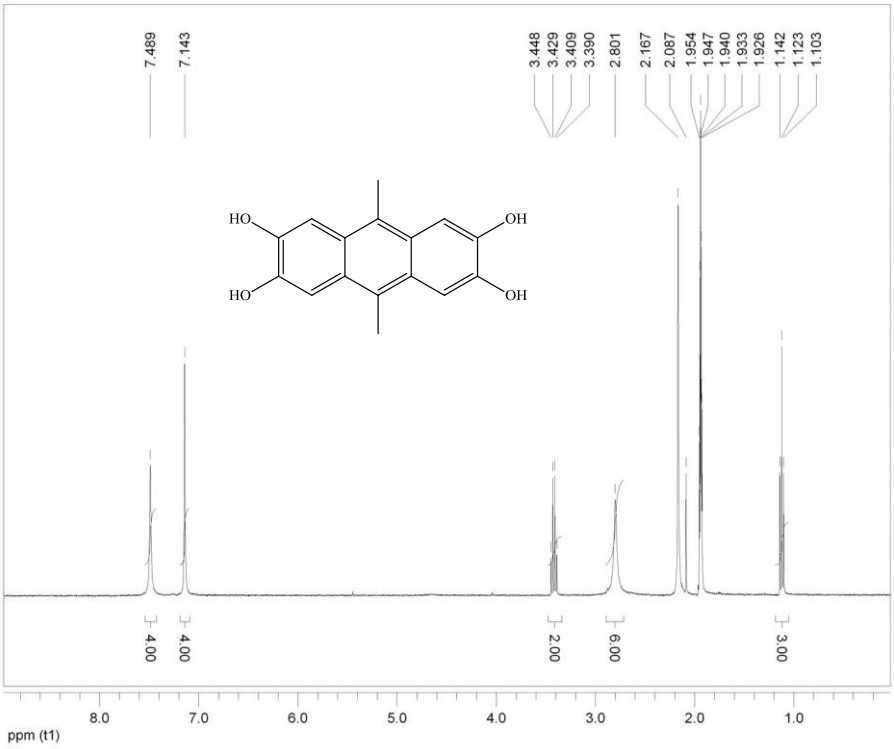
7.489
7.143
3.448
3.429
3.409
3.390
2.801
2.167
2.087
1.954
1.947
1.940
1.933
1.926
1.142
1.123
1.103
HO
OH
HO
OH
4.00
4.00
2.00
6.00
3.00
8.0
7.0
6.0
5.0
4.0
3.0
2.0
1.0
ppm (t1)

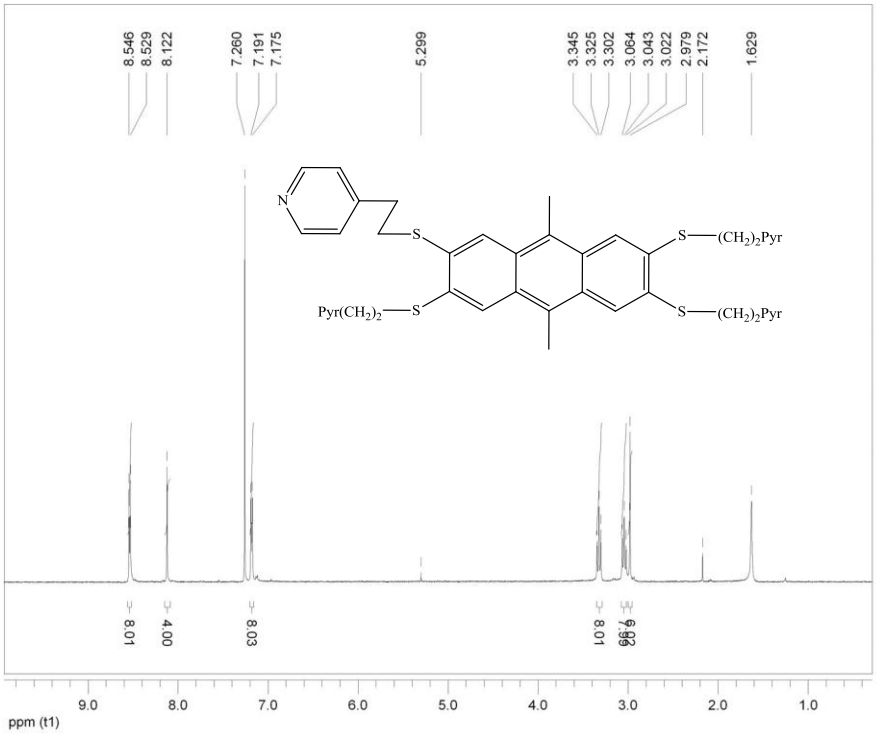
8.546
8.529
8.122
7.260
7.191
7.175
5.299
3.345
3.325
3.302
3.064
3.043
3.022
2.979
2.172
1.629
N
S
S—(CH2)2Pyr
Pyr(CH2)2—S
S—(CH2)2Pyr
8.01
4.00
8.03
8.01
9.0
8.0
7.0
6.0
5.0
4.0
3.0
2.0
1.0
ppm (t1)

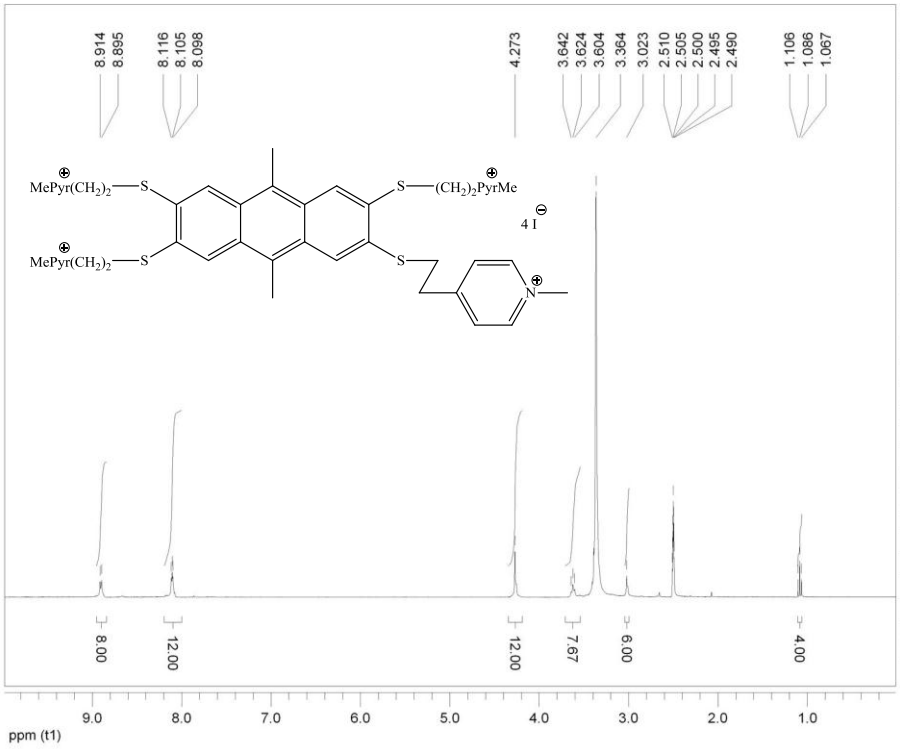
8.914
8.895
8.116
8.105
8.098
4.273
3.642
3.624
3.604
3.364
3.023
2.510
2.505
2.500
2.495
2.490
1.106
1.086
1.067
MePyr(CH2)2—S
S—(CH2)2PyrMe
4 I
8.00
12.00
12.00
7.67
6.00
4.00
9.0
8.0
7.0
6.0
5.0
4.0
3.0
2.0
1.0
ppm (t1)

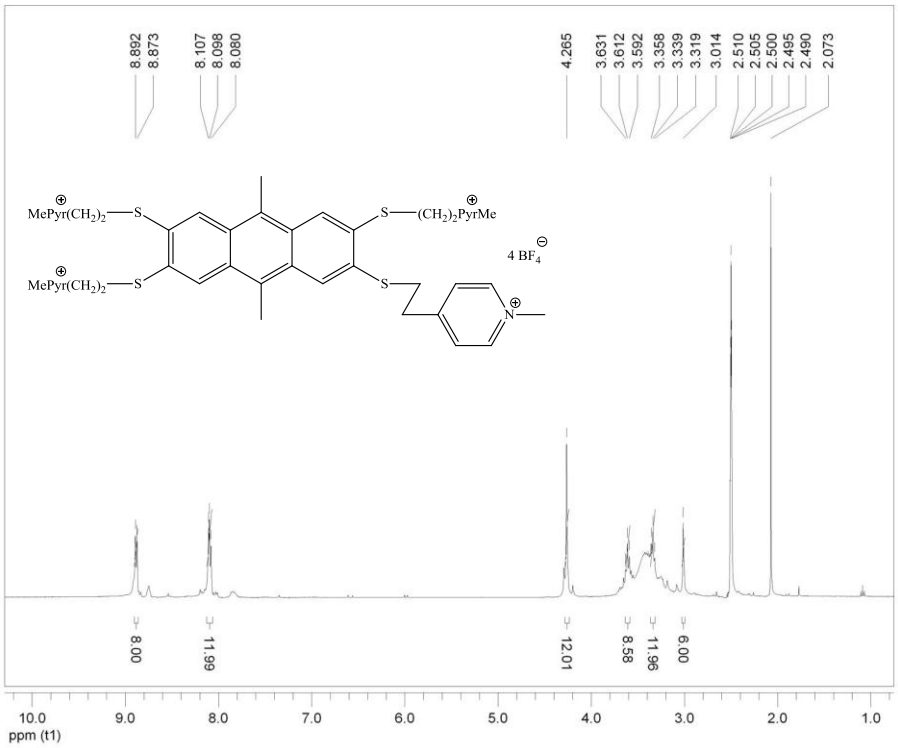
8.892
8.873
8.107
8.098
8.080
4.265
3.631
3.612
3.592
3.358
3.339
3.319
3.014
2.510
2.505
2.500
2.495
2.490
2.073
MePyr(CH2)2—S
S—(CH2)2PyrMe
4 BF4
8.00
11.99
12.01
8.58
11.96
6.00
10.0
9.0
8.0
7.0
6.0
5.0
4.0
3.0
2.0
1.0
ppm (t1)

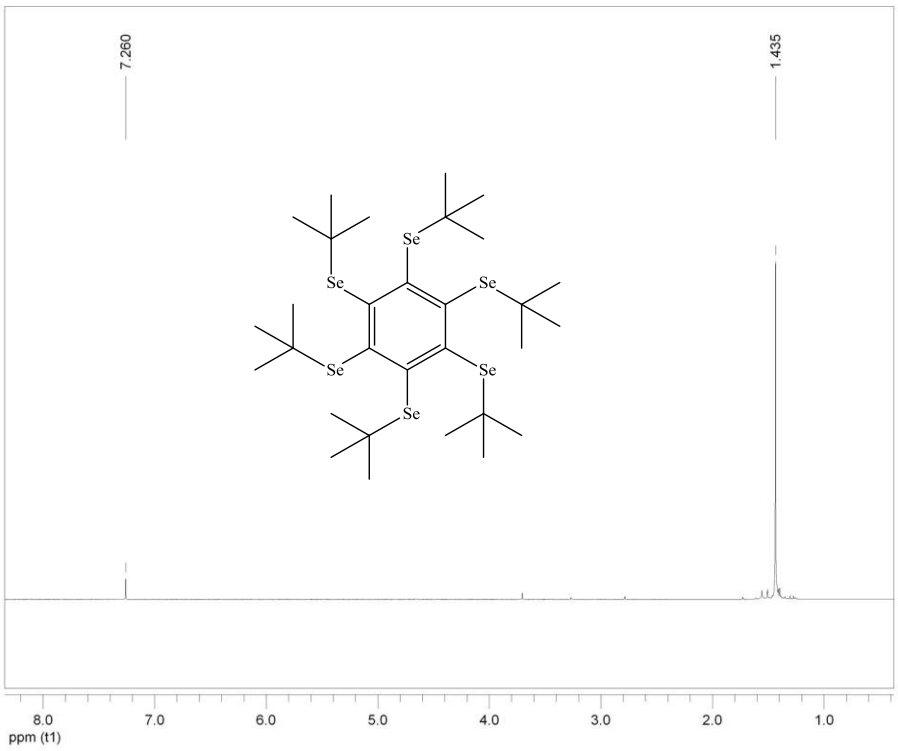
7.260
1.435
Se
Se
Se
Se
Se
Se
8.0
7.0
6.0
5.0
4.0
3.0
2.0
1.0
ppm (t1)